We would like to thank the two anonymous referees for their careful reading of the manuscript, and also the time they dedicated to evaluating this study. All comments were highly insightful. Please find below our point-by-point response to the critiques and a highlight to the changes made to the manuscript to address these. For ease of discussion, we have continuously numbered the reviewer's comments. Our responses are shown using blue color, and we strongly feel that we were able to address all the points raised.

RESPONSES TO COMMENTS OF ANONYMOUS REFEREE #1

1. I know it is kind of tradition of the "Grenoble" group to classify the ice core data into summer and winter values and there might be circumstances were this is justified. However, this is always difficult, since the record does not contain clear time markers for the seasons and therefore assumptions have to be made. In this case, the 25th and 75th percentiles of thickness of an annual layer were arbitrarily chosen, assuming equal distribution of precipitation (and preservation on the glacier) throughout the year. This is conducted without explaining the hypothesis behind.

We agree with the reviewer's point that classifying the ice core data into summer (or warm season) and winter (or cold season) values was done without clear time markers. However, the ELB ice cores show very clear seasonality with the high summer values and the low winter values of water stable isotopic composition ($\delta^{18}O$ and dD) and NH_4^+. Both $\delta^{18}O$ and NH_4^+ were thus used to classify seasonal ice layers of the cores (summer-half year and winter-half year). We think our proposed method for dating and seasonality is the best one for the moment.

We also agree with the reviewer's point that the 25th and 75th percentiles of thickness of a seasonal snow layer were chosen in this study assuming equal distribution of precipitation through a year and the hypothesis behind choosing this method is not clearly explained.

In the Caucasus region, most of the annual precipitation occurs in the western and southern sections of the Caucasus, reaching 3240 mm y^{-1} at Achishkho weather station (1880 m). Precipitation ranges between 2000 and 2500 mm y^{-1} at 2500 m a.s.l. in the west and declines to 800–1150 mm y^{-1} in the east on the northern slope of the Caucasus (Mikhalenko et al., 2015). A regular year round precipitation has been observed in the Western Caucasus at Klukhorskiy Pereval station (2037 m a.s.l., 50 km westward; the location is indicated with number "7" in Kozachek et al., 2016, Fig. 1), where the proportions of mean summer and winter precipitations are 0.94 m (52%) and 0.87 m (48%), respectively, and precipitation of each month accounts for 6-11 % of total precipitation for the period 1966-2009 (www.meteo.ru). In our 2009 ELB core, the mean annual snow accumulation rate (1455 mm w.e. y^{-1} for the last 140 years) obtained by counting annual layers suggests that the deposited snow at the ELB site is well preserved without significant loss driven by wind erosion, although direct precipitation measurements are not available at the drilling site. Seasonal snow is also well preserved, with nearly equal deposition amounts from the warm season (45% of total

accumulation) and the cold season (55% of total accumulation), e.g., a short firn core spanning the years 2012-2009 (Kutuzov et al., 2013). Hence, we suggest that it was reasonable to assume that precipitation at the ELB site is equally distributed through a year.

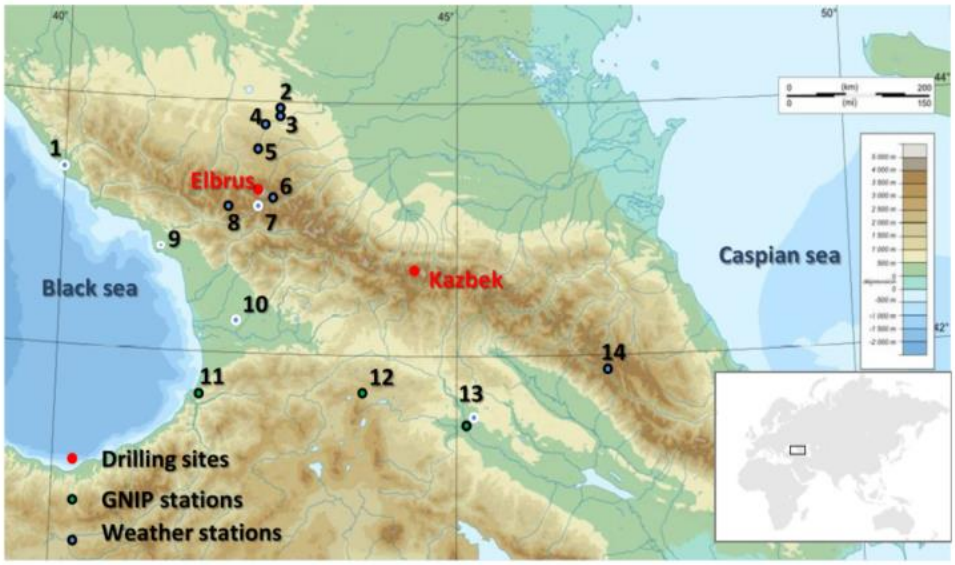

Fig. 1: Map showing the region around Elbrus (black rectangle in the world's map in the lower right corner), with shading indicating elevation (m above sea level). Drilling sites are indicated with red filled circles, GNIP stations as green filled circles, and meteorological stations as blue dots. Stations situated to the south of the Main Caucasus Ridge according to the precipitation cycle pattern are shown using a blue dot with white outside circle and the stations situated to the north are displayed with black outside circle (see text for the details). The number of the various stations refers to Table 1 for their detailed description.

Figure 1. Map showing the region around Elbrus (black rectangle in the world's map in the lower right corner). Drilling sites are indicated with red filled circles, GNIP stations as green filled circles, and meteorological stations as blue dots. Klukhorskiy Pereval station is indicated with number "7". (from Kozachek et al., 2016).

Furthermore, our separation method of seasonal snow layers is supported by the coincidence of maximum (or minimum) values of both $\delta^{18}O$ and NH^{4+} in the annual snow layers. Most of maximum (or minimum) values of both $\delta^{18}O$ and NH^{4+} were observed in the 25th and 75th percentiles of thickness of a summer (winter) snow layer. However, we also observed unusual shift in NH_4^+ from $\delta^{18}O$ pattern, although it was rarely observed (roughly 10-year-ice layers over the entire 198-year-long record). The impact of inaccurate seasonal separation on rBC was limited by calculating median rBC mass seasonal concentration values.

We finally concluded that the 25th and 75th percentiles of thickness of a seasonal snow layer were chosen in this study assuming equal distribution of precipitation through a year and that summer or winter rBC mass concentrations that were provided following this method are corresponding to summer maximum or winter minimum values of climate proxies in an annual layer.

We added a following sentence in line 150:

"This seasonal separation method is fairly supported by the fact that (i) observed precipitation in the Western Caucasus is equally distributed throughout a year (e.g., at Pereval Klukhorskiy observatory which is located at 2037 m a.s.l. and only 50 km from the drilling site: 52% of the annual precipitation (resp. 48%) is observed during summer (resp. winter) and each monthly precipitation accounts for 6-11 % of total precipitation for the period 1966-2009; www.meteo.ru) and (ii) maximum or minimum values of both $\delta^{18}O$ and NH_4^+ coincide for most of the Elbrus core annual ice layers."

2. The obtained summer and winter rBC records do show similar trends and the slight differences around 1900 are not discussed at all.

As indicated by the reviewer, we observed slight increase of winter rBC values in 1900-1920 with respect to summer rBC values. We do not fully understand why the seasonal differences were shown in the period 1900-1920. There might be increased winter BC inputs for the period transporting to the ELB site. We used BC emission inventory data of Lamarque et al. (2010), which are well supported by rBC deposition reconstructed from Greenland ice cores (McConnell et al., 2007). In McConnell et al. (2007), rBC particles that transported from North America markedly increased at the beginning of 20th century, indicating increased BC emissions in North America for the period. The enhanced BC input from North America might be detected in the ELB ice core layers of the period 1900-1920, although it was not shown in our simulations.

The following sentence was added in line 254.
"Meanwhile, the slight increase of winter rBC values in 1900-1920 with respect to summer rBC values are not well understood. Although speculative, it may reflect increased winter BC inputs transporting through the free troposphere (FT) from North America, where BC emissions markedly increased at the beginning of 20th century"

3. As expected the JJA and DJF scenarios for the atmospheric BC load are different, with much higher contributions from North America (NAM) to DJF. However, the authors do not question their summer and winter classification in the ice core because of this finding, but do instead explain the difference with an overestimation of the NAM footprint density by the simulation. To my opinion, the classification into JJA and DJF needs better justification, for example by showing that the annual ice core rBC concentrations and annual atmospheric BC loads agree less.

Unlike scenario results for the seasonal atmospheric BC load at the ELB site, the seasonal rBC trends of the ELB ice cores were similar except for the periods 1900-1920 and 2000-2013. The winter rBC increased relatively for the first case and the summer rBC increased more obviously for

the latter case. Both features were not shown in the simulations. Particularly, the increased winter rBC concentrations in ~1900-1920 may be linked with stronger BC inputs from North America at the beginning of the 20th century when the BC emissions were the strongest in that region. We do not understand well the mechanisms by which North American BC emissions could be strongly detected in the ELB ice core for this period.

The following sentence was added in line 406.

"Consequently, the observed overestimation of NAM contribution for winter at the ELB site (Fig 9b) is likely due to an overestimation of NAM footprint density in the statistical process applied on FLEXPART simulation data, although the stronger BC inputs from NAM might have contributed to the increased winter rBC concentrations of the ELB ice core at the beginning of 20th century."

Unfortunately, anthropogenic BC emissions from ACCMIP are available on the decadal scale only. We thus cannot show annual atmospheric BC load.

4. What is puzzling is that in the other manuscript about this ice core (Kozachek et al., CPD 2016), classification into seasons is conducted by introducing the mean delta18O value as threshold. If at all, the procedure should be the same. Please also reconcile the details about the core (20.4 m here, 20.5 m in Kozachek et al.; dating uncertainty few years here, +- 1 year in Kozachek et al.) and include a reference to that manuscript.

Mikhalenko et al. (2015) has established age scale of the ELB ice core using NH_4^+ and succinic acid, and posteriori validation with $\delta^{18}O$, resulting in a 2-year difference between annual layer counting of $\delta^{18}O$ signal and the NH_4^+ stratigraphy at 106.7 m. Kozachek et al. (2016) has made the ice core dating using annual $\delta^{18}O$, $\delta^{18}O$ threshold, and use of NH_4^+ and succinic acid if issues with $\delta^{18}O$. They initially reported a 1-year uncertainty of the dating but recently corrected this estimate to 2-years to agree with Mikhalenko et al. (2015)(see response to reviwers provided by Kozachek et al. (2016), TCD) . Finally, both Mikhalenko et al. (2015) and Kozachek et al. (2016) have reported that a 2-year difference between annual layer counting of $\delta^{18}O$ signal and the NH_4^+ stratigraphy at 106.7 m. This is an excellent agreement on age scales that were obtained by two methods, suggesting robust dating results of the ELB ice core from top to 106.7 m.

In our study, we discussed rBC annual variability down to 156.6 m, corresponding to year 1825. the dating uncertainty from the surface to 106.7 m is 2-years as indicated by Mikhalenko et al. (2015) and Kozachek et al. (2016), but the uncertainty may be larger below 106.7 m due to ice thinning.

We corrected in line 141:

"The dating uncertainty is 2-year between 106.7 m and the top (Kozachek et al., 2016; Mikhalenko et al., 2015) and probably larger below 106.7 m due to ice thinning"

We corrected in line 72:

".. a 20.5 m-long ice core (the 2013 core)…"

5. The rBC size distribution data are very valuable since they support other findings that the rBC particle sizes in snow and ice are larger than in the atmosphere. However, the difference in MMD between summer and winter (Fig. 5) is not so obvious to me. The main discrepancy is for the few data points before 1960 where the data coverage is anyway poor. Have you tested if the MMDs for the period after 1960 are significantly different, considering the strong variability of the data?

We agree with the reviewer's point that the difference in MMD between summer and winter is not very obviously shown. We thus conducted student's t-test on the MMD between summer and winter for the period 1960-2009 and the test resulted in significantly different mean MMD values between two seasons with $p<0.01$. On the other hand, summer (or winter) MMDs for two periods for which highly variable rBC concentrations were observed, e.g., the period 1960-1999 and the period 2000-2009, were not significantly different.

The following sentence was added in line 285:

"No statistically significant temporal change in rBC MMD was identified over the 1940-2009 period."

The following sentence was added in line 302:

"The difference in seasonal rBC size distributions are statistically significant ($p<0.01$)."

6. Line 63: rephrase: that is reconstructed in the downstream of Europe.

The sentence revised as follow: "The ice core record therefore provides information on long-term variability and evolution of BC emissions of Europe."

7. Line 95: Please specify "upper section" (move this up from line 116).

The "upper section" in the sentence was specified as follow:

"The upper section of the 2009 firn core (surface to 7.2 m depth) was analyzed discretely."

The firn depth in line 221 was revised to 7.2 m.

8. Line 117: Give max and min numbers of data points per year.

We added max and min numbers of data points per year in line 117:

"The density of rBC data points per year (N=8~376) depends on annual snow accumulation rates

and ice thinning with depth."

9. Lines 211-214: The fact that biomass burning emissions frequently occur in summer should be reflected in the emission estimates. I do not understand the argument for not considering the biomass emissions in DJF.

We agree with the reviewer's point that the argument why biomass burning emissions were considered only for summer simulations is not clear. ACCMIP inventory (Lamarque et al., 2010) provides anthropogenic BC emissions on a decadal scale and biomass burning (savanna and forest burnings) BC emissions on a monthly scale. The figure below, which is a part of Saehee LIM's PhD dissertation, shows that biomass burning BC emissions ($kg/m^2/s$) in Europe that were calculated by ACCMIP were frequent in summer time and minimized in winter time. The biomass burning BC emissions in May to August are larger by two orders of magnitude than those in November to February.

This is now clearly stated in the sentence in line 213 as follow: "
"We used anthropogenic emission only for constraining BC emissions in DJF and both anthropogenic and biomass burning emissions for constraining BC emissions in JJA, because seasonal biomass burning BC emissions are maximized in summer time (May to August), being two orders of magnitude larger than during winter time (September to February), as respect to anthropogenic emissions occurring year-round (Lamarque et al., 2010)."

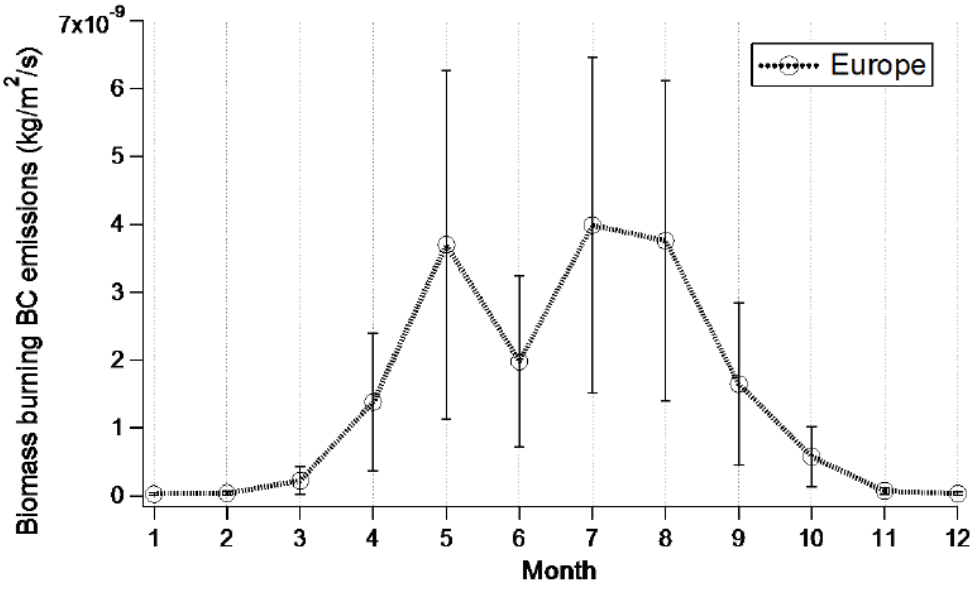

Figure I-10. Seasonality of BC emissions from biomass burning in Europe. The biomass burning BC emissions here include emissions from savanna burning and forest fires during the period 1900 to 2000. Mean monthly BC emissions with one standard deviation are estimated from ACCMIP BC emission inventory. Sources are from Lamarque et al. (2010).

10. Lines 232-236: Include Jungfraujoch (e.g. Bukowiecki et al., Aerosol and Air Quality Research, 16: 764–788, 2016).

The reference (Bukowiecki et al., 2016) was added with relevant discussion in lines 232-236. In line 231, the following sentence is added. "In contrast to the boundary layer sites, the atmospheric measurements at high-elevation sites in Europe (e.g., Puy de Dôme at 1465 m a.s.l., Sonnblick at 3106 m a.s.l. and Jungfraujoch at 3580 m a.s.l.) revealed 2 to 3 times higher EC levels during summer than winter (Bukowiecki et al., 2016; Pio et al., 2007; Venzac et al., 2009), "

11. Line 293: Mikhalenko et al. (2015) do not mention aerosol removal processes. Please clarify that you assume that wet deposition dominates, since there is often and regular precipitation throughout the year.

We agree with the reviewer's point that Mikhalenko et al. (2015) did not mention aerosol removal processes and the line 293 in our manuscript can be misleading. We therefore corrected the sentence as follow:

"The shift of rBC sizes induced by dry deposition should be negligible, as quite high (100-200 mm/month) and fairly constant precipitation rate throughout the year near the drilling site (e.g., 52%

and 48% of annual precipitation observed in summer and winter, respectively, at Klukhorskiy Pereval station (2037 m a.s.l., 50 km westward; Kozachek et al., 2016) suggests that wet deposition can be the dominant aerosol removal pathway at this site."

12. Line 355: Matthias, 2004: Is this Matthias and Bösenberg, 2002?

The reference "Matthias, 2004" in line 355 should be "(Matthias et al., 2004)" and the relevant reference info should be revised.

Matthias et al. (2004) showed regular lidar observations of the vertical aerosol distribution at 10 European Aerosol Research Lidar Network (EARLINET) stations since 2000, for which they used the planetary boundary layer (PBL) height (km asl) at each station. Two mountain stations (L'Aquila at 1742 m agl and Potenza at 1536 m agl) showed monthly mean PBL height above 2 km asl and often higher weakly PBL height up to 3 km asl, while the PBL height was lower with monthly mean PBL of 1-2 km asl at the other stations. Thus, simulations for summer particle footprint within the lower 2 km layer in the atmosphere performed in our study are fairly consistent to the real PBL height at an area surrounding mountain and realistic aerosol transport to the drilling site.

13. Figure 2 would benefit from a better quality map. Please indicate location of ELB and explain abbreviations in the figure (NAM etc).

Figure 2 was replaced with a better quality map as follow. The location of ELB is indicated by a red circle symbol.

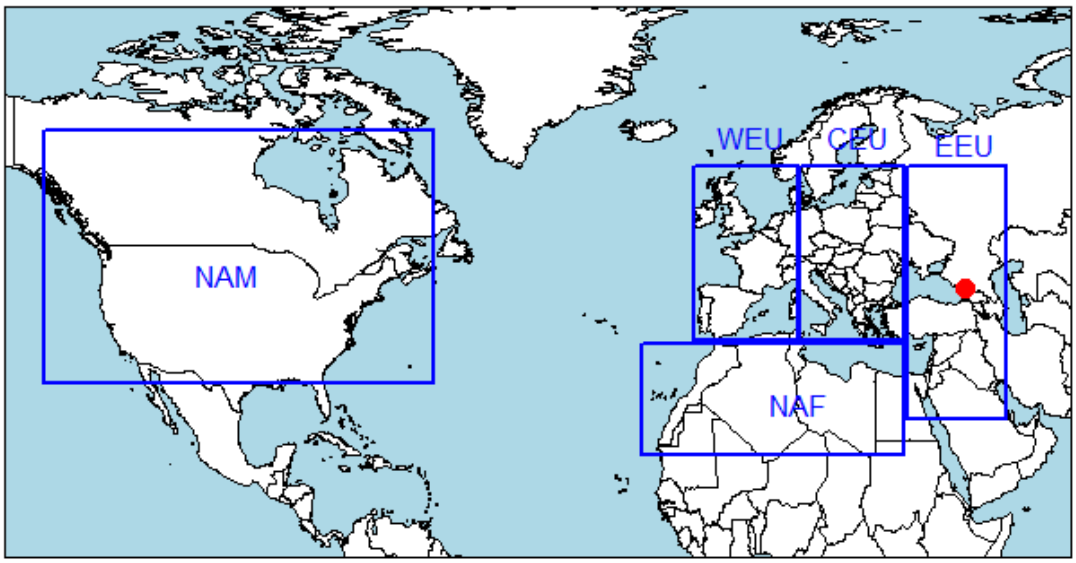

Figure 2. Five sub-regions classified as potential rBC emission source regions. Elbrus drilling site (43°20'53,9"N, 42°25'36,0"E) is indicated by a red circle. WEU, CEU, EEU, NAF and NAM represent Western Europe, Central Europe, Eastern Europe, North Africa and North America, respectively.

14. Fig. S1: The overlap between the 2009 and 2013 cores is not convincing. Could you support this with other ice core parameters (e.g. stable isotopes)?

An overlapping section (m w.e.) of the 2013 core and the 2009 core was described with water stable isotope (δ18O) values in the following figure. The common δ18O values were observed in the 2013-core depth of 6.8-10.7 m w.e., corresponding to year 2009-2007. The current Fig. S1 was replaced with the following figure.

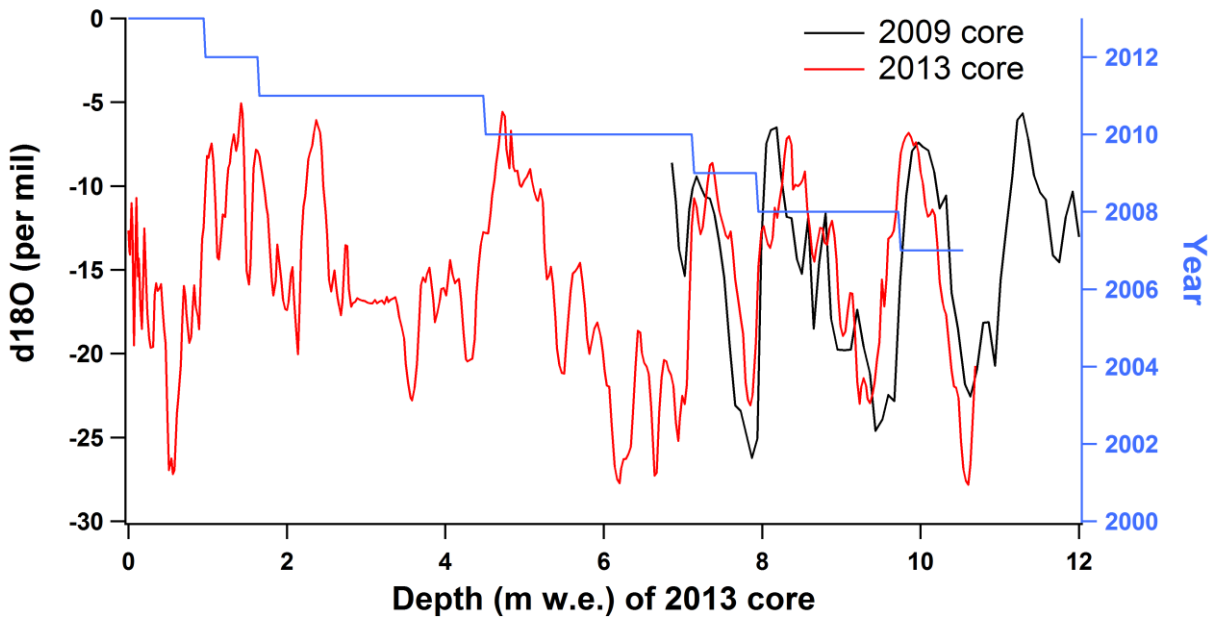

Figure S1. An overlapping section of the 2009 core and the 2013 core. We used the common d18O feature dated year 2009-2007 and located at 7-11 m w.e. depth along the 2013-core depth scale to extend the 2009-core record (main core) with the 2013-core record.

RESPONSES TO COMMENTS OF ANONYMOUS REFEREE #2

15 I agree with the comment of Referee #1 about the summer/winter layers subdivisions. If possible, I will recommend reinforcing the rBC-based annual layers determination with some other seasonally varying parameters, such as water stable isotopes, thus being in agreement with the other paper about the Elbrus ice core (Kozachek et al., CPD 2016).

See reply to similar comment (#4) from reviewer #1.

In addition, we added to the manuscript annual rBC variability (10^{th}, 50^{th} and 90^{th} percentile values of annual snow layer; following figure) in Fig. 4c with relevant description.

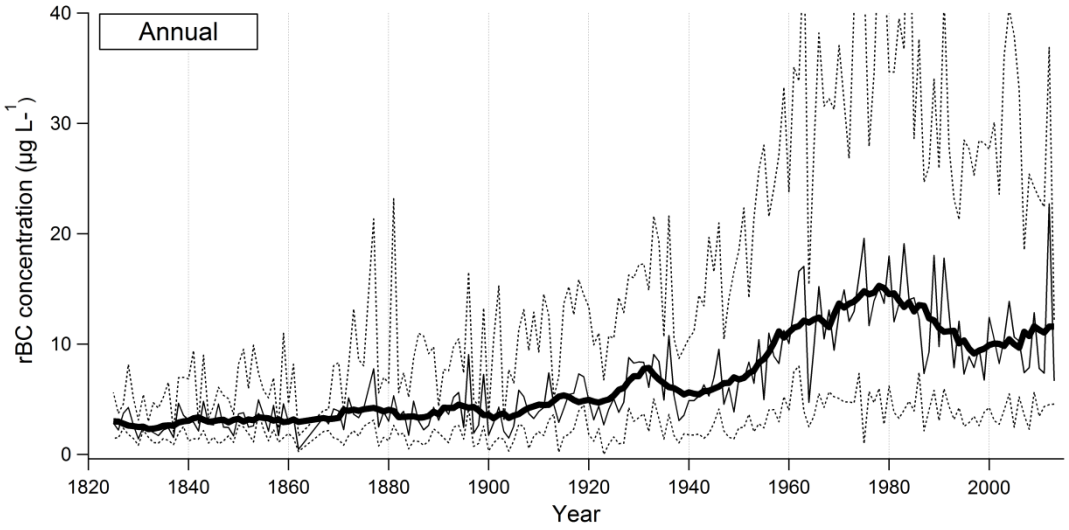

Figure 4c. Annually averaged temporal evolution in rBC mass concentration of the ELB ice cores. Thin solid line is medians and dashed lines are lower and upper 10th percentiles of the annual rBC values. Thick line is 10-year smoothing of medians.

16. I have found the rBC particles' MMD time series and the related interpretation very interesting and promising. I agree with all the interpretations but, however, the seasonality is not clear since the 1960s; particularly, during the 1980s the winter MMDs are even larger than the summer ones. I don't think that the difference between summer and winter is statistically significant in the period 1960-2010, can you please add some comments and interpretations about that? Or at least describe the MMD time series more in details.

See reply to similar comment (#5) from reviewer #1.

17. Line 37: it's better to write: "to be transported" instead of "to transport".

It is rewritten to "to transport".

18. Line 38: "In high-altitude or –latitude areas ": missing word?

Yes, "high" prior to "-latitude area" is missing. "In high-altitude or –latitude areas " in line 38 is thus revised to "In high-altitude or high–latitude areas ".

19. Line 39: "that may accelerate": it's better to write, "in accelerating".

It is rewritten to "in accelerating".

20. Line 47: “proximity”: how much? It’s better to specify for the sake of clarity.

We agree with the reviewer. European Alpine sites such as Col du Dôme, Colle Gnifetti and Fiescherhorn are approximately ~100 km away from big cities such as Lyon, France, Milano, Italy and Geneva, Switzerland, respectively. The sentence in line 47 was revised to “Particularly, the geographical proximity of the ice cores at high-altitude Alpine sites, e.g., European Alpine sites such as Col du Dôme, Colle Gnifetti and Fiescherhorn (Jenk et al., 2006; Legrand et al., 2007; Thevenon et al., 2009) to densely populated regions (approximately ~100 km) allows us to observe…”.

21. Line 50: please add a phrase regarding the BC/EC relation and write that there aren’t other rBC records in this region.

This is an important point: we agree that terminology of BC derived from different methods should be differentiated. We thus add a sentence in line 53 as follow:
“It should be noted that EC refers to data derived from thermal methods which are different than optical methods providing BC (including rBC derived from incandescence methods) (Petzold et al., 2013)”.
In line 63, we now stress that the ELB ice core rBC record is the first rBC record retrieved over Europe as follow: “For the first time, a high resolution, continuous rBC record is extracted from an ice core over Europe. The Elbrus rBC record thus brings new and unique information on long-term variability and evolution of BC European emissions.”

22. Line 102: “Nd YAG laser”: please write “Nd:YAG laser”, with colon.

It is revised.

23. Line 123: “single rBC”, I will add “particle”.

“single rBC” is replaced with “single rBC particle” as recommended.

24. Line 198: you may want to underline that the procedure is the same as for the entire atmospheric column.

This is a good point. We added a sentence in line 198:

"…, while the simulation procedure is the same as for the entire atmospheric column".

25. Line 228: try to be clearer, e.g. "The highest rBC mass concentrations were observed: : :"

For clarity, the sentence was revised to "The highest rBC mass concentration of an annual snow layer was observed in summer snow layer".

26. Line 236: substitute "consistent to: : :" with "consistent with: : :"

It is revised as recommended.

27. Line 259: if you write and compare the absolute values for the EC with you rBC analyses it will be better to write something about the conversion factor also in this part of the paper, or at least specify "how" to compare the values explicitly.

This is an excellent point: we agree that the most accurate and clear way to compare the absolute values for the EC of CDD and CG cores with for our rBC of ELB cores is describing corrected values based on existing lab experiments to evaluate different methods (Thermal (or thermal-optical) method vs. SP2-based incandescence method). Previously, Lim et al. (2014) conducted inter-comparison of the SP2-based incandescence method and thermal-optical method (EUSAAR2 protocol) for different field samples (i.e., Elbrus firn core, CDD snow fit, Greenland summit firn and Himalayan snow). In the experiments, Lim et al. (2014) found that thermal-optical method had disadvantages for providing accurate EC mass concentrations because (i) filtration efficiency, that is necessary prior to thermal-optical method, was strongly dependent on BC particle size and OC loading on the filter, (ii) presence of dust can cause negative EC artifact and (iii) OC pyrolyzation can biase OC/EC split point and then generally cause a positive EC artifact. On the other hand, the rBC results of SP2-based method was dependent on the SP2 gain setting that determines lower and upper rBC size limits. As a results, EC/rBC ratios were 0.5±0.2 for CDD snow pit and 1.0±0.4 for ELB firn core, and the results came from mixed factors such as particle morphology and chemical composition of the field samples. We thus conclude that describing the comparison of our ELB rBC with previously measured EC of CDD and CG cores using corrected values or conversion factor may cause another uncertainty because we do not know BC or EC size and chemical composition (amount of OC and amount/type of dust) of the ELB, CDD and CG cores. Therefore we added a sentence in line 264 of the manuscript about why direct comparison of the ELB rBC with the EC of CDD and CG should be made with caution. We will further add a reference, Lim et al. (2014) at the end of the sentence to guide readers.

28. Line 293: please clarify why dry deposition is not playing a significant role in the rBC particles diameter changing.

Black Carbon particles are deposited in snow by either wet (i.e., in precipitation) or dry deposition. In general, BC removal from the atmosphere by wet deposition is estimated to be 3 times more efficient compared to dry deposition processes (Bauer et al., 2013). However, in some regions, dry deposition is considered to be the main process (or relatively more important than in other regions) for BC removal in the atmosphere (e.g., Khumbu valley in the Himalayas, Bonasoni et al. (2010); Yasunari et al. (2010). As discussed in replies to comment (#1) and (#11) we expect wet deposition to be the main deposition process at the ELB site, with an equal distribution along the year. Hence, it is reasonable to assume that BC deposition processes at the ELB site do not vary strongly along the seasons, and mainly involve wet removal by precipitation. We cannot quantify the proportion of dry deposited BC aerosols in snow, but this dry deposition effect should not be higher in specific month or season because observed monthly or seasonal precipitation rate is regular (e.g., at Klukhorskiy Pereval station).

Once deposited, in addition to wind drift and erosion, particles can experience sublimation (snow to water vapor transition) or snow melt (Ginot et al., 2001; Schotterer et al., 2001). These postdeposition processes might affect BC concentrations and/or morphology within the snowpack. Only few studies have investigated how post-deposition processes impact BC in snow (Hagler et al., 2007a, 2007b). Hagler et al. (2007b) showed relatively conservative behavior of EC in the 4-year snow pit layers at Summit, Greenland, where summer snow melting is limited similar to the ELB site, while water-soluble and –insoluble OC would undergo substantial post-depositional processing. Hence, it is reasonable to assume that post deposition processes are not impacting BC on snow at the ELB site.

29. Line 295: should surface snow melting modify the rBC size distribution? Explain and add references.

To our knowledge, we do not know the studies of relationship between snow melting and rBC size modification. But there are plenty of studies showing that snow melt increase snow grain size. We first mentioned that ".. post-deposition processes are thus not expected to alter rBC size distributions." in line 295. We revised this sentence as follow:

"Similarly, significant snow melt was not observed in the ELB summer ice layers. Although there is a lack of studies about the impact of snow melting on rBC size distribution, such processes would not be expected at the ELB drilling site"

30. Line 332: can you exclude the surface snow melting effect in increasing the rBC MMD in the 2003 summer layer? Please explain.

The 2003 summer ice layer shows a clear shift on rBC MMD, which we attributed to influence of particle deposition from biomass burning plumes. This 2003 summer snow layer experienced some melting (Kozachek et al., 2016), but we can rule out that such melting is driving the unusual MMD signal described above. We actually observed others snow layers with melting event (e.g., summer layers of year 2001 and year 2000), and all of these event did not show any anomalies of rBC MMD toward larger values.

31. Line 386: "BC depositing to snow": "BC depositing ON snow".

It was corrected.

32. Line 462: "as new a proxy": write "as a new proxy".

It was corrected.

33. For what concern the figures I would personally prefer having the deepest and the oldest parts always on the right or on the left (but this is up to you).

We drew the figure by both methods, but finally decided the current one, because two of three papers that reported the alpine EC records (Jenk et al., 2006; Legrand et al., 2007; Thevenon et al., 2009) showed the figure of the past EC variability having the deepest parts on the left. We thus followed the method to help readers to compare their EC and our rBC records.

References

Bauer, S. E., Bausch, A., Nazarenko, L., Tsigaridis, K., Xu, B., Edwards, R., Bisiaux, M. and McConnell, J.: Historical and future black carbon deposition on the three ice caps: Ice core measurements and model simulations from 1850 to 2100, J. Geophys. Res. Atmos., 118(14), 7948–7961, doi:10.1002/jgrd.50612, 2013.

Bonasoni, P., Laj, P., Marinoni, A., Sprenger, M., Angelini, F., Arduini, J., Bonafè, U., Calzolari, F., Colombo, T., Decesari, S., Di Biagio, C., di Sarra, A. G., Evangelisti, F., Duchi, R., Facchini, M., Fuzzi, S., Gobbi, G. P., Maione, M., Panday, A., Roccato, F., Sellegri, K., Venzac, H., Verza, G., Villani, P., Vuillermoz, E. and Cristofanelli, P.: Atmospheric Brown Clouds in the Himalayas: first

two years of continuous observations at the Nepal Climate Observatory-Pyramid (5079 m), Atmos. Chem. Phys., 10(15), 7515–7531, doi:10.5194/acp-10-7515-2010, 2010.

Bukowiecki, N., Weingartner, E., Gysel, M., Collaud Coen, M., Zieger, P., Herrmann, E., Steinbacher, M., Gäggeler, H. W. and and Baltensperger, U.: A Review of More Than 20 Years of Aerosol Observation at the High Altitude Research Station Jungfraujoch, Switzerland (3580masl), Aerosol Air Qual. Res., 16(3), 764–788, doi:10.4209/aaqr.2015.05.0305, 2016.

Ginot, P., Kull, C., Schwikowski, M., Schotterer, U. and Gäggeler, H. W.: Effects of postdepositional processes on snow composition of a subtropical glacier (Cerro Tapado, Chilean Andes), J. Geophys. Res. Atmos., 106(D23), 32375–32386, doi:10.1029/2000jd000071, 2001.

Hagler, G. S. W., Bergin, M. H., Smith, E. A. and Dibb, J. E.: A summer time series of particulate carbon in the air and snow at Summit, Greenland, J. Geophys. Res., 112(D21), D21309, doi:10.1029/2007JD008993, 2007a.

Hagler, G. S. W., Bergin, M. H., Smith, E. A., Dibb, J. E., Anderson, C. and Steig, E. J.: Particulate and water-soluble carbon measured in recent snow at Summit, Greenland, Geophys. Res. Lett., 34(16), L16505, doi:10.1029/2007GL030110, 2007b.

Jenk, T. M., Szidat, S., Schwikowski, M., Gaggeler, H. W., Brutsch, S., Wacker, L., Synal, H. A. and Saurer, M.: Radiocarbon analysis in an Alpine ice core: record of anthropogenic and biogenic contributions to carbonaceous aerosols in the past (1650-1940), Atmos. Chem. Phys., 6, 5381–5390, doi:10.5194/acp-6-5381-2006, 2006.

Kozachek, A., Mikhalenko, V., Masson-Delmotte, V., Ekaykin, A., Ginot, P., Kutuzov, S., Legrand, M., Lipenkov, V. and Preunkert, S.: Large-scale drivers of Caucasus climate variability in meteorological records and Mt Elbrus ice cores, Clim. Past Discuss., 1–30, doi:10.5194/cp-2016-62, 2016.

Kutuzov, S., Shahgedanova, M., Mikhalenko, V., Ginot, P., Lavrentiev, I. and Kemp, S.: High-resolution provenance of desert dust deposited on Mt. Elbrus, Caucasus in 2009–2012 using snow pit and firn core records, Cryosph., 7(5), 1481–1498, doi:10.5194/tc-7-1481-2013, 2013.

Lamarque, J.-F., Bond, T. C., Eyring, V., Granier, C., Heil, A., Klimont, Z., Lee, D., Liousse, C., Mieville, A., Owen, B., Schultz, M. G., Shindell, D., Smith, S. J., Stehfest, E., Van Aardenne, J., Cooper, O. R., Kainuma, M., Mahowald, N., McConnell, J. R., Naik, V., Riahi, K. and van Vuuren, D. P.: Historical (1850–2000) gridded anthropogenic and biomass burning emissions of reactive gases and aerosols: methodology and application, Atmos. Chem. Phys., 10(15), 7017–7039, doi:10.5194/acp-10-7017-2010, 2010.

Legrand, M., Preunkert, S., Schock, M., Cerqueira, M., Kasper-Giebl, A., Afonso, J., Pio, C., Gelencsér, A. and Dombrowski-Etchevers, I.: Major 20th century changes of carbonaceous aerosol components (EC, WinOC, DOC, HULIS, carboxylic acids, and cellulose) derived from Alpine ice cores, J. Geophys. Res., 112(D23), D23S11, doi:10.1029/2006jd008080, 2007.

Lim, S., Faïn, X., Zanatta, M., Cozic, J., Jaffrezo, J.-L., Ginot, P. and Laj, P.: Refractory black carbon mass concentrations in snow and ice: method evaluation and inter-comparison with elemental carbon measurement, Atmos. Meas. Tech., 7(10), 3307–3324, doi:10.5194/amt-7-3307-2014, 2014.

Matthias, V., Balis, D., Bösenberg, J., Eixmann, R., Iarlori, M., Komguem, L., Mattis, I., Papayannis, A., Pappalardo, G., Perrone, M. R. and Wang, X.: Vertical aerosol distribution over Europe: Statistical analysis of Raman lidar data from 10 European Aerosol Research Lidar Network (EARLINET) stations, J. Geophys. Res., 109(D18), D18201, doi:10.1029/2004JD004638, 2004.

McConnell, J. R., Edwards, R., Kok, G. L., Flanner, M. G., Zender, C. S., Saltzman, E. S., Banta, J. R., Pasteris, D. R., Carter, M. M. and Kahl, J. D. W.: 20th-century industrial black carbon emissions altered arctic climate forcing, Science (80-.)., 317(5843), 1381–1384, doi:10.1126/science.1144856, 2007.

Mikhalenko, V., Sokratov, S., Kutuzov, S., Ginot, P., Legrand, M., Preunkert, S., Lavrentiev, I., Kozachek, A., Ekaykin, A., Faïn, X., Lim, S., Schotterer, U., Lipenkov, V. and Toropov, P.: Investigation of a deep ice core from the Elbrus western plateau, the Caucasus, Russia, Cryosph., 9(6), 2253–2270, doi:10.5194/tc-9-2253-2015, 2015.

Petzold, A., Ogren, J. A., Fiebig, M., Laj, P., Li, S.-M., Baltensperger, U., Holzer-Popp, T., Kinne, S., Pappalardo, G., Sugimoto, N., Wehrli, C., Wiedensohler, A. and Zhang, X.-Y.: Recommendations for reporting “black carbon” measurements, Atmos. Chem. Phys., 13(16), 8365–8379, doi:10.5194/acp-13-8365-2013, 2013.

Schotterer, U., Stichler, W. and Ginot, P.: The influence of post-depositional effects on ice core studies: Examples from the Alps, Andes, and Altai, 2001.

Thevenon, F., Anselmetti, F. S., Bernasconi, S. M. and Schwikowski, M.: Mineral dust and elemental black carbon records from an Alpine ice core (Colle Gnifetti glacier) over the last millennium, J. Geophys. Res., 114, doi:D17102 10.1029/2008jd011490, 2009.

Yasunari, T. J., Bonasoni, P., Laj, P., Fujita, K., Vuillermoz, E., Marinoni, A., Cristofanelli, P., Duchi, R., Tartari, G. and Lau, K.-M.: Estimated impact of black carbon deposition during pre-monsoon season from Nepal Climate Observatory-Pyramid data and snow albedo changes over Himalayan glaciers, Atmos. Chem. Phys., 10(14), 13, doi:10.5194/acp-10-6603-2010, 2010.

Black carbon variability since preindustrial times in Eastern part of Europe reconstructed from Mt Elbrus, Caucasus ice cores

Saehee Lim[1, *], Xavier Faïn[1], Patrick Ginot[1, 2], Vladimir Mikhalenko[3], Stanislav Kutuzov[3], Jean-Daniel Paris[4], Anna Kozachek[3] and Paolo Laj[1, 2]

1 Univ. Grenoble-Alpes, CNRS, Institut des Géosciences de l'Environnement, Grenoble, France.

2 Univ. Grenoble-Alpes, CNRS, IRD, Observatoire des Sciences de l'Univers, Grenoble, France.

3 Institute of Geography, Russian Academy of Sciences, Moscow, Russia.

4 Laboratoire des Sciences du Climat et de l'Environnement, IPSL, CEA-CNRS-UVSQ, CE Orme des Merisiers, 91190 Gif sur Yvette, France.

*now at: Department of Earth and Environmental Sciences, Korea University, Seoul, South Korea.

Corresponding to: S. Lim (saehee.lim@gmail.com)

Abstract Black carbon (BC), emitted by fossil fuel combustion and biomass burning, is the second largest man-made contributor to global warming after carbon dioxide (Bond et al., 2013). However, limited information exists on its past emissions and atmospheric variability. In this study, we present the first high-resolution record of refractory BC (rBC, including mass concentration and size) reconstructed from ice cores drilled at a high-altitude Eastern European site in Mt. Elbrus (ELB), Caucasus (5115 m a.s.l.). The ELB ice core record, covering the period 1825-2013, reflects the atmospheric load of rBC particles at the ELB site transported from the European continent with a larger rBC input from sources located in the Eastern part of Europe. In the first half of the 20th century, European anthropogenic emissions resulted in a 1.5-fold increase in the ice core rBC mass concentrations as respect to its level in the preindustrial era (before 1850). The summer (winter) rBC mass concentrations increased by a 5-fold (3.3-fold) in 1960-1980, followed by a decrease until ~2000. Over the last decade, the rBC signal for summer time slightly increased. We have compared the signal with the atmospheric BC load simulated using past BC emissions (ACCMIP and MACCity inventories) and taken into account the contribution of different geographical region to rBC distribution and deposition at the ELB site. Interestingly, the observed rBC variability in the ELB ice core record since the 1960s is not in perfect agreement with the simulated atmospheric BC load. Similar features between the ice core rBC record and the best scenarios for the atmospheric BC load support that anthropogenic BC increase in the 20th century is reflected in the ELB ice core record. However, the peak in BC mass concentration observed in ~1970 in the ice core is estimated to occur a decade later from past inventories. BC emission inventories for the period 1960s-1970s may be underestimating European anthropogenic emissions. Furthermore, for summer time snow layers of the last 2000s, the slightly increasing trend of rBC deposition likely reflects recent changes in anthropogenic and biomass burning BC emissions in the Eastern part of Europe. Our study highlights that the past changes in BC emissions of Eastern Europe need to be considered in assessing on-going air quality regulation.

1 Introduction

Climate forcing of black carbon (BC), a primary aerosol emitted by fossil fuel and biomass combustions, is of

great concern due to its strong light-absorbing ability and small size allowing it to ~~be~~ transport over long distances (Bond et al., 2013; Ramanathan and Carmichael, 2008). In high-altitude or high-latitude areas, BC has been identified as a significant contributor in accelerating snowmelt (Hansen and Nazarenko, 2004; Xu et al., 2016). Despite numerous studies through both measurements and model simulations (Bond et al., 2013 and references therein), little is known about BC's past variability, e.g., before year 2000, and sensitivity to climate change primarily due to limited in-situ atmospheric BC measurements both temporally and spatially (Collaud Coen et al., 2007, 2013).

Reconstruction of atmospheric BC variability from ice core archives can thereby be very helpful to understand past BC emissions and provide additional constraint on BC emission inventories (Bisiaux et al., 2012a; Kaspari et al., 2011; Legrand et al., 2007; McConnell et al., 2007; Wang et al., 2015). Particularly, the geographical proximity of the ice cores at high-altitude Alpine sites, e.g., European Alpine sites such as Col du Dôme, Colle Gnifetti and Fiescherhorn (Jenk et al., 2006; Legrand et al., 2013; Thevenon et al., 2009) to densely populated regions (approximately ~100 km) –allows us to observe a fingerprint of BC emissions and past temporal variability in the anthropogenic source regions. In this respect, elemental carbon (EC) records reconstructed from ice cores at Western European Alpine sites (Col du Dôme and Colle Gnifetti) highlight a pronounced EC increase starting mid-20th century (Legrand et al., 2007; Thevenon et al., 2009) with increasing anthropogenic activity in the Western Europe (Fagerli et al., 2007; Lamarque et al., 2010). It should be noted that EC refers to data derived from thermal methods which are different than optical methods providing BC (including rBC derived from incandescence methods) (Petzold et al., 2013). –However, recent EC records over the last two decades are not available from these Western European ice cores, which makes it difficult to quantify historic BC emissions and thus provide implications for assessing European air quality regulation initiated since 1970 (Tørseth et al., 2012; Vestreng et al., 2007). Furthermore, long-term ice core BC records have never been reconstructed from the Eastern European regions where even atmospheric measurements are relatively scarce (Pio et al., 2007; Yttri et al., 2007). Reconstruction of BC records with a wide range of coverage both temporally and spatially is crucial to understand BC emission properties and establish regulations on the emissions.

In this study, we present a high-resolution record of refractory BC (rBC) deposition to snow at a high-altitude site in Mt. Elbrus, Caucasus (5115 m a.s.l.) covering the period 1825-2013. Located between the Black and the Caspian seas, Mt. Elbrus is influenced by prevailing westerly from the European continent (Mikhalenko et al., 2015). For the first time, a high resolution, continuous rBC record was extracted from an ice core over Europe. The Elbrus rBC record thus brings new and unique information on long-term variability and evolution of BC European emissions. The study documents the variability of rBC deposition and provides a comparison with the expected atmospheric BC variability based on past emission inventories also considering atmospheric transport to the drilling site.

2. Method

2.1 Ice core drilling site

A 181.8 m-long ice core (the 2009 core) was drilled at the Western Plateau of Mt. Elbrus (ELB), the highest summit of the Caucasus (43°20'53,9"N, 42°25'36,0"E, 5115 m a.s.l.) (Figure 1) on September 2009. In addition, a 20.5 m-long ice core (the 2013 core) was extracted in June 2013 at the same site to expand the existing ice-core

sample set from 2009 to 2013. Drilling was performed in a dry borehole with a lightweight electromechanical drilling system, and was accompanied by borehole temperature measurements. Borehole temperatures ranged from -17 °C to 10 m depth to -2.4 °C at 181 m of the 2009 core (Mikhalenko et al., 2015).

The core were packed in polyethylene sealed bag and stored on the glacier at -10°C. After the drilling campaign, the core were packed in insulated core boxes and shipped frozen to the cold laboratory of the Lomonosov Moscow State University for preliminary investigation and water stables isotopes analyzes. In Moscow, the core was split and one-half was shipped to LGGE (Laboratoire de Glaciologie et Géophysique de l'Environnement - now Institut de Géophysique de l'Environnement) in Grenoble, France for additional analyzes.

2.2 rBC ice core analysis

The top 156.6 m of the 2009 core and the entire 2013 core were analyzed at LGGE in 2013-2014 and in 2014, respectively, using an ice core melter system coupled with a jet nebulizer (APEX-Q, Elemental Scientific Inc., Omaha, NE) and a single particle soot photometer (SP2, Droplet Measurement Technologies, Boulder, Colorado). We have used the terminology proposed by Petzold et al. (2013) for incandescence-based BC measurements. Our results are therefore reported in terms of refractory-BC (rBC). It should be noted that there is a direct relationship (although not necessarily linear) between rBC and BC measured with other techniques (Kondo et al., 2011a; Laborde et al., 2012; Miyakawa et al., 2016).

Dust and conductivity are continuously analyzed simultaneously to rBC. Briefly, ice core sticks (3.4 cm x 3.4 cm x 1 m) were melted at a mean rate of 3 cm min^{-1} and the melt water from the inner 6.8 cm^2 of the sticks were continuously collected. After de-bubbling, the sample flow is split to rBC analytical line with a mean flow of about 70±10 µL min^{-1}. The flow rate dedicated to rBC analyses is continuously recorded using a mass flow meter (SENSIRION© SLI-2000). In parallel, the melt water was sampled by two auto-samplers at the end of the CFA for off-line ionic species analysis and archive storage. The upper section of the 2009 firn core (surface to 7.2 m depth) was analyzed discretely.

Ice core rBC analysis using the SP2 has been reported previously (Bisiaux et al., 2012a, 2012b; Ginot et al., 2014; Jenkins et al., 2013; Kaspari et al., 2014; Wang et al., 2015). Specifically, recent papers describe detailed analytical evaluation for rBC in liquid samples, e.g., rain, snow and ice core, using the SP2 (Lim et al., 2014; Mori et al., 2016; Schwarz et al., 2012; Wendl et al., 2014). The SP2 uses a laser-induced incandescence method to measure the mass of individual rBC particle (Schwarz et al., 2006; Stephens et al., 2003). Briefly, an individual rBC particle passes through the laser beam intra-cavity of a 1,064 nm Nd:YAG laser and incandescences. Of two PMT-photo detectors (broad and narrow bands) that are used to detect incandescence signal, we used only broadband detector to derive rBC mass avoiding low signal-to-noise ratio from the narrowband detector. The SP2 was calibrated by analyzing mass-selected fullerene soot (Alfa Aesar Inc., USA). The design and gain settings of our SP2 resulted in the lower and upper limit of measurements for rBC mass to be ~0.3-220 fg. A particle larger than 220 fg was treated as the particle of 220 fg. Loss of rBC particles occurring during aerosolization in the APEX-Q was calibrated and corrected daily by rBC standard solutions (Aquadag®, Acheson Inc., USA; 8 steps from 0.1 to 100 µg L^{-1}), which resulted in rBC mass recovery of 75±7 %. The rBC fraction that was not aerosolized was partially identified in drains and internal surface of the APEX-Q (see Supplementary information in Lim et al. (2014)). To prevent contamination and achieve the rBC levels as low as

possible, both an instrumental blank (ultrapure water) and a 5-cm procedure blank (frozen ultrapure water cut in the cold room) were run daily prior to field sample analysis, until the rBC counting reached 0 to 1 per second, equivalent to rBC concentration of less than 0.01 μg L^{-1}.

High resolution continuous rBC data recorded every second was smoothed at a depth resolution of 1 cm, except the upper section (surface to 7.2 m depth) of the 2009 core that was discretely analyzed at a depth resolution of ~5-10 cm. The density of rBC data points per year (N=8~376) depends on annual snow accumulation rates and ice thinning with depth. The two ice cores are overlap for snow layers of year 2007-2009 (Fig. S1). The records described here for rBC concentrations are (i) the 2009 ice core from 2.9 m to 156.6 m, corresponding to calendar years of 1825-2008 and (ii) the top 15.9 m of the 2013 core, corresponding to calendar years of 2009-2013. These two ice core records cover the calendar years of 1825-2013.

As a first survey for long-term rBC size distributions of ice core record, mass equivalent diameter of measured single rBC particle, D_{rBC}, was calculated, assuming a void-free BC density of 1.8 g cm^{-3} (Moteki and Kondo, 2010). The calculated D_{rBC} was in the range of ~70 and 620 nm. A series of test using mono-dispersed polystyrene latex (PSL) spheres with known diameters (150-600 nm) and poly-dispersed standard BC (Aquadag®) suggests that the APEX-Q/SP2 system preserves original size information of rBC particles in liquid samples and provides highly reproducible rBC size measurements with a variation of < 5 nm (Sect. 2.2.3 and 2.2.5 in Lim et al., 2014; Wendl et al., 2014). rBC size distributions were retrieved seasonally and simplified with a log-normal fit with a bin size (#)=200. Mass mode diameter (MMD) of the log-normal fit was then extracted to further reduce parameters. Size intervals between bin channels vary, with the minimum interval of less than 8 nm for the MMD 200-350 nm. Here, all SP2 data were processed with the SP2 toolkit developed by M. Gysel at the Paul Scherrer Institute (PSI, Switzerland; http://aerosolsoftware.web.psi.ch/).

2.3 Ice core dating and seasonal signature

Ice core dating was determined by counting annual layers from 1825 to 2013 using the seasonal cycles of ammonium (NH_4^+), succinic acid and water stable isotopes (δD and $\delta^{18}O$) that were analyzed discretely. Based on the examination of the ammonium and succinic acid profiles, each annual layer was divided into two parts corresponding to snow deposition under winter condition and summer condition (Legrand et al., 2013; Mikhalenko et al., 2015; Preunkert et al., 2000). In addition, the annual layer counting was further confirmed using the reference horizon from a tritium peak (1963) and a volcanic horizon (Katmai in 1912). The mean annual net accumulation rate of 1455 mm w.e. for the last 140 years was estimated from these proxies. The dating uncertainty is 2-year between the top and 106.7 m (Kozachek et al., 2016; Mikhalenko et al., 2015) and probably larger below 106.7 m due to ice thinning. - Further details about dating are found in Mikhalenko et al. (2015).

Ice core seasonality was determined by the ammonium stratigraphy and further verified by the isotope variations. However, seasonal separation of the high-resolution rBC record made by lower-resolution ammonium profile was sometimes challenging particularly at the edge of two seasons, misleading winter (summer) rBC layers to be more concentrated (less concentrated) by the adjacent seasonal rBC layer. To avoid inaccurate separation of an annual ice layer into winter and summer intervals, only mid-summer and mid-winter rBC concentrations were extracted by considering data comprised between the 25th percentile and the 75th percentile of the depth thickness

of each seasonal snow layer. This seasonal separation method is fairly supported by the fact that (i) observed precipitation in the Western Caucasus is equally distributed throughout a year (e.g., at Klukhorskiy Pereval station located 2037 m a.s.l., 50 km westward from the drilling site: 52% of the annual precipitation (resp. 48%) is observed during summer (resp. winter) and each monthly precipitation accounts for 6-11 % of total precipitation for the period 1966-2009; www.meteo.ru) and (ii) maximum or minimum values of both $\delta^{18}O$ and ammonium coincide for most of the Elbrus core annual ice layers. The mid-summer and mid-winter are therefore corresponding roughly to the warmest three months and the coldest three months ("background winter") of a year. Later in the manuscript, summer and winter of this study will refer to mid-summer and mid-winter, respectively.

2.4 Atmospheric transport modeling

2.4.1 Model description and runs

FLEXPART v6.2 lagrangian particle dispersion model (LPDM) calculates the trajectories of tracer particles using the mean winds interpolated from the gridded analysis field and parameterizations representing turbulence and convective transport (Forster et al., 2007; Stohl and Thomson, 1999). FLEXPART was run using reanalysis fields of the European Centre for Medium-Range Weather Forecasts (ECMWF, ERA-Interim) at 0.75°×0.75° resolution, which is available since 1979. Here, a backward simulation mode was used to analyze particles transport pathways from potential flux regions to the sampling site (Seibert and Frank, 2004; Stohl et al., 2005). To limit computational cost, simulations were performed for two selected periods: 2005-2009 and 1979-1983. We selected these periods because: (i) year 1979 is the first year of ECMWF data and year 2009 is the last year of our longer ice core (2009 ice core) that were analyzed prior to the 2013 ice core and (ii) these years are inflections in rBC trends (Sect. 3.2). It would thus be sufficient to analyze transport patterns influencing rBC at ELB and determine potential changes in these transport patterns. 1,000 particles are released at the drilling site during every 5-day interval in June to August (JJA) and in December to February (DJF). Modelled global average atmospheric lifetimes of BC particles varies by a factor of more than 3, ranging from 3 to 10 days (Bond et al., 2013). Because BC particles reaching the high-altitude ELB site would experience longer lifetimes than the particles transporting in the planetary boundary layer (PBL), simulations were performed using a BC lifetime of 5-, and 7-day. However, 7-day air mass trajectories were extending to the Pacific and therefore made little difference with the 5 days simulations. Thus we set the BC lifetime as 5-day. Number of particles were then computed every 3h at 0.5°×0.5° resolution.

2.4.2 Sensitivity by potential source regions

The finally defined footprint density F (i, j, n) is expressed as a parameter encompassing released particle number and residence time along the particles pathway, in procedure defined unit (p.d.u.). This final result is theoretically identical to potential emission sensitivity (PES), called source-receptor-relationship by Seibert and Frank (2004), which is proportional to the particle residence time in a particular grid cell with a fixed altitude range.

To facilitate analysis we reduced the number of variables from the gridded footprint density by summing them

over large regions. We classified the footprint areas into five geographical regions with specific rBC emission sources (Figure 2). The regions identified are as follows: **EEU** (Eastern Europe including nearby the Mt. Elbrus, Ukraine and Europe Russia and a part of Middle East), **CEU** (Central Europe), **WEU** (Western Europe), **NAF** (North Africa), **NAM** (North America) **and Others** (The Atlantic and a part of Northern Europe above 60°N).
To display our results, we first calculate the footprint density *F*e of the entire footprint area:

$$Fe\ (i,j) = \sum_{n=1}^{N} F(i,j,n)$$

Here, $F\ (i, j, n)$ is footprint density, where i and j are the indices of the latitude/longitude grid and n runs over the total number of cases N. *F*e indicates the entire footprint area where the aerosols track during the last 5 days of transport. Note that we found little inter-annual variability in the footprint contribution of each region to the ELB site with a 3 % variation over the two periods (2005-2009 and 1979-1983). Assuming that this inter-annual variability in footprint density is not large enough to influence on long-term rBC trends and the results over the two periods are thus fairly representative of 20th century, we combined the simulations results and used this approach to study long-term emission contribution of each geographical region to rBC distribution and deposition at our drilling site.
In addition to the calculation using total particles in the atmospheric column, calculations using particles positioned in the lowest 2 km layers in the atmosphere were performed to investigate emission source regions of aerosols transporting from low altitudes, while the simulation procedure is the same as for the entire atmospheric column. To show the potential particle transport strength of each region relative to the entire area, we calculated the percentages of the footprint density in each region relative to the one in the entire area. To do this, we sum *F*e (i, j) over the entire footprint area resulting in one value. In the same way, we sum $F\ (i, j)$ within each of the five regions resulting in five values.

2.5 Historic BC emission inventories

To describe temporal variability in the regional BC emissions and atmospheric load of BC transported to the ELB site, we used time-varying anthropogenic and biomass burning BC emissions estimated by ACCMIP (Emissions for Atmospheric Chemistry and Climate Model Intercomparison Project) inventory for the period 1900-2000 on the decadal scale (at 0. 5°×0. 5° resolution; Lamarque et al., 2010) and MACCity (MACC/CityZEN EU projects) inventory for the year 2008 (at 0. 5°×0. 5° resolution; Diehl et al., 2012; Granier et al., 2011; Lamarque et al., 2010; van der Werf et al., 2006). Note that the ACCMIP inventory provide decadal means (e.g., '1980' corresponds to the mean of 1980-1989) for the biomass burning estimates and representative values (e.g., '1980' is a representative of 1975-1985) for the anthropogenic estimates, leading to 5-year shift between two estimates. We used anthropogenic emission only for constraining BC emissions in DJF and both anthropogenic and biomass burning emissions for constraining BC emissions in JJA, because seasonal biomass burning BC emissions are maximized in summer time (May to August), being two orders of magnitude larger than during winter time (September to February), as respect to anthropogenic emissions occurring year-round (Lamarque et al., 2010).

3 Results and discussion

3.1 High resolution rBC record from Elbrus ice cores

We present the first high-resolution rBC record of ice cores drilled in the Mt. Elbrus, Caucasus (2009 and 2013 cores, Figure 3a). The rBC concentrations along the two cores ranged from 0.01 μg L^{-1} to 222.2 μg L^{-1} with a mean±1σ of 11.0±11.3 μg L^{-1} and a median of 7.2 μg L^{-1}. A 20-m long section is zoomed in Figure 3b to highlight the higher resolution of rBC signals when continuously recorded at 1-cm depth interval compared to the surface snow and firn section (from top to 7.2 m) analyzed discretely at ~5-10 cm-depth interval. The rBC record was found to preserve sub-annual variability from top to depth of 156.6 m with rBC spikes reflecting large and abrupt variability in deposition of atmospheric rBC particles. Such high-resolution record brings new opportunities to study dynamic atmospheric vertical transport and/or sporadic events in a season.

A well-marked seasonal rBC cycle (e.g., Fig 3b) was characterized for the 2013 core and the 2009 core down to 156.6 m by consistent high summer values ranging from 0.2 to 222.2 μg L^{-1} with a mean±1σ of 15.5±12.9 μg L^{-1} and a median of 11.7 μg L^{-1} and low winter values ranging from 0.2 to 44.6 μg L^{-1} with a mean±1σ of 5.9±5.1 μg L^{-1} and a median of 4.5 μg L^{-1} (Table 1). The highest rBC mass concentration of an annual snow layer was observed in summer snow layer. In atmospheric observations at ground-based sites in Western and Central Europe boundary layer, EC aerosol mass concentrations in winter are higher roughly by a factor of 2 than in summer mainly due to the enhanced domestic heating (Pio et al., 2007; Tsyro et al., 2007). In contrast to the boundary layer sites, the atmospheric measurements at high-elevation sites in Europe (e.g., Puy de Dôme at 1465 m a.s.l., Sonnblick at 3106 m a.s.l. and Jungfraujoch at 3580 m a.s.l.) revealed 2 to 3 times higher EC levels during summer than winter (Bukowiecki et al., 2016; Pio et al., 2007; Venzac et al., 2009), ~~and Jungfraujoch at 3580 m a.s.l.) revealed 2 to 3 times higher EC levels during summer than winter (Bukowiecki et al., 2016; Pio et al., 2007; Venzac et al., 2009),~~ reflecting the efficient upward transport of BC aerosols from the polluted boundary layer to the high-altitudes during summer, primarily by thermally-driven convection and thickening boundary-layer height (Lugauer et al., 1998; Matthias and Bösenberg, 2002). This is consistent with the rBC seasonality observed in the ELB ice core.

3.2 Long term evolution of rBC mass concentrations

Time series of seasonal (summer and winter) and annual medians of rBC mass concentrations from 1825 to 2013 are shown in Figure 4. Medians are shown with lower and upper 10th percentiles to illustrate rBC concentrations. The rBC concentrations varied significantly over the past ~190 years with a large inter-annual variability. Summer, winter and annual rBC medians increased gradually since the onset of 20th century with a rapid increase in ~1950 lasting until ~1980. 10-year moving averaged rBC values reached their maximums in the 1960s and 1970s.

Concentrations and relative change to levels of preindustrial era (here, defined as 1825-1850) for given time periods are summarized in Table 1. For the period of 1825-1850, median (± standard deviation, SD) of rBC concentrations were 4.3±1.5 μg L^{-1} in summer and 2.0±0.9 μg L^{-1} in winter. The rBC concentrations increased by a ~1.5-fold in 1900-1950. Meanwhile, the slight increase of winter rBC values in 1900-1920 with respect to summer rBC values are not well understood. Although speculative, it may reflect increased winter BC inputs

transporting through the free troposphere (FT) from North America, where BC emissions markedly increased at the beginning of 20th century (Lamarque et al., 2010; McConnell et al., 2007). -Over the period of 1960-1980, rBC concentrations increased by a factor of 5.0 in summer and a factor of 3.3 in winter. The larger relative change of summer rBC than one of winter for the period suggests that rBC emissions in summer source region increased more sharply for this time period. Notably, in addition to medians, the lower 10th percentiles of both summer and winter rBC increased since the preindustrial era, highlighting that rBC background level in the atmosphere at ELB was also significantly modified. Meanwhile, upper 10th percentiles ranged up to 75 μg L^{-1}, 35 μg L^{-1} and 56 μg L^{-1} for summer, winter and annual variability, respectively.

Of the EC records available in the Western European mountain glaciers, only Col du Dôme (hereafter, CDD; Legrand et al., 2007) and Colle Gnifetti (hereafter, CG; Thevenon et al., 2009) summer records provide EC records for the recent time (until ~1990 and 1980, respectively), whereas the Fiescherhorn (hereafter, FH; Jenk et al., 2006) record is available until 1940 only. Both summer records at CDD and CG show somewhat comparable preindustrial EC levels (~2 μg L^{-1} for CDD and ~7 μg L^{-1} for CG in the mid-1800s) to the ELB rBC (4.3±1.5 μg L^{-1} in 1825-1850) and substantially increased EC concentrations for the period 1950-1980 since the mid-19th century, similar to the ELB rBC. This suggests that EC emissions show a common trend at the European scale, and that such trend has been recorded in the different European high-altitude ice cores from CDD, CG, and ELB. Some differences, such as peak time period and increase/decrease rate between records that may reflect sub-regional (e.g., Western Europe vs. Eastern Europe) emission changes, may be also noteworthy. However, direct comparison of the ELB rBC with the Western European ice core records should be made with caution owing to both (i) different analytical methods applied for the ice cores (e.g., ELB rBC: APEX-Q/SP2, CDD EC: thermal-optical method with EUSAAR2 protocol, and CG EC: thermal method) (Lim et al., 2014) and (ii) lower data resolution particularly for the CDD core (a few data points for a decadal EC concentration). We thus focus on evaluating the ELB rBC record in Sect. 3.5 by comparing with simulated atmospheric load of BC particles that were transported from source regions to the Mt. Elbrus.

3.3 Past variability in rBC size distributions

The first record of temporal and seasonal changes in rBC size distribution was extracted from the ELB ice core. Mass equivalent diameter of rBC particles (D_{rBC}) was log-normally distributed. The mode of rBC mass size distributions (mass mode diameter, MMD) was determined for both summer and winter layers by fitting a log-normal curve to the measured distribution (e.g., Figure S2). This approach provides reliable results of representative rBC size in seasonal ice layers as the determined MMDs fall into the measured size range (~70-620 nm).

Figure 5 shows time series of rBC MMD for the period of 1940 to 2009. The upper and lower limits of the periods selected for retrieving rBC MMD were chosen so as a large number of rBC particles in the seasonal ice layer would be available and would allow to secure reliable size distribution of the ice layer. Faster melting of snow layers of year 2010-2013 and thinner ice layers below the layer of year 1940 did not allow to record sufficient numbers of rBC particles and thus robust rBC size distributions could not be retrieve. For the considered time period, rBC MMD of both summer and winter layers varied ranging from 207.3 nm to 378.3 nm with a geometric mean of 279.4±1.1 nm. No statistically significant temporal change in rBC MMD was

identified over the 1940-2009 period.

Notably, rBC particles measured in this study show the MMD shifted to larger sizes than those measured in the atmosphere over Europe (MMD of 130-260 nm) (Dahlkötter et al., 2014; Laborde et al., 2013; Liu et al., 2010; McMeeking et al., 2010; Reddington et al., 2013), even larger than atmospheric rBC diameter measured at an high alpine site, Jungfraujoch (JFJ) in Switzerland (MMD of 220-240 nm) (Liu et al., 2010). The shift of rBC sizes induced by dry deposition should be negligible, as quite high (100-200 mm/month) and fairly constant precipitation rate throughout the year near the drilling site (e.g., 52 % and 48 % of annual precipitation observed in summer and winter, respectively, at Klukhorskiy Pereval station (see Sect. 2.3)) suggests that wet deposition can be the dominant aerosol removal pathway at this site. Similarly, significant snow melt was not observed in the ELB summer ice layers. Although there is a lack of studies about the impact of snow melting on rBC size distribution, such processes would not be expected at the ELB drilling site. Rather, the different rBC size distributions of the ice core from those in the atmosphere are likely associated with removal process of rBC particles during precipitation. Recent study using the SP2 technique showed the rBC size distribution in rainwater shifted to larger sizes (MMD= ~200 nm) than that in air (MMD= ~150 nm) in Tokyo, indicating that large rBC particles were more efficiently removed by precipitation (Mori et al., 2016). The preferential wet removal of larger rBC particles (Mori et al., 2016; Moteki et al., 2012) could reasonably explain the larger MMD of rBC particles observed in the ice core than atmospheric rBC aerosols (Schwarz et al., 2013).

The difference in seasonal rBC size distributions was statistically significant ($p<0.01$). In summer, the MMD varied ranging from 227.4 nm to 378.3 nm with a geometric mean of 290.8±1.1 nm (Fig.5, red curve). In winter, the MMD varied ranging from 207.3 nm to 344.9 nm with a geometric mean of 268.7±1.1 nm (Fig.5, blue curve). The rBC MMD of summer ice layers tended to be slightly larger than that of winter layers. Despite few observational evidences, we hypothesize that larger rBC size in summer may reflect advection of rBC aerosols transported from the PBL by thermally-driven convection, while in winter aerosols transported in the FT could be smaller due to longer residence time in the atmosphere and accordingly, more chances for larger aerosols to be removed by precipitation prior to reaching the ELB site. Our hypothesis seems to be reasonable being consistent to the findings of in-situ aerosol measurements at high-altitude sites in Europe. Liu et al. (2010) found that rBC aerosols at JFJ were slightly larger when the site was influenced by valley sources, anthropogenic pollutants from lower altitudes. Submicron aerosol size distributions were also overall shifted to larger size in summer (50 to 150 nm) than in winter (below 50 nm) at European mountain stations with altitude of ~1000-3000 m a.s.l. (Asmi et al., 2011). The authors in the latter explained this feature by relatively polluted air masses from the PBL during daytime in summer, but more influence of the FT air masses in winter. Similar to the clear seasonal cycle in rBC mass concentration, the clear seasonal rBC size distributions of the ELB ice core point out seasonal differences in origins of air masses reaching the ELB drilling site: PBL air with less chance of aerosol wet removal in summer and the free tropospheric air in winter.

In addition, the larger rBC MMD in summer layers can be associated with specific summer sources of atmospheric rBC particles, such as forest fires and/or agricultural fires. Particularly, forest fires in Southern Europe and agricultural fires in Eastern Europe may well contribute to summer aerosol loading in Europe (Bovchaliuk et al., 2013; van der Werf et al., 2010; Yoon et al., 2011). Previous SP2 studies have reported the larger size of rBC aerosols for biomass burning plumes, e.g., MMD of ~200 nm (Kondo et al., 2011b; Schwarz et al., 2008; Taylor et al., 2014) compared to rBC sizes for urban plumes. In the ELB ice core, we observed a

maximum rBC MMD of 378.3 nm, with a maximum rBC mass concentration of 222.2 μg L^{-1} in the late summer snow layer of year 2003, when extreme forest fire events occurred over the Iberian Peninsula and the Mediterranean coast (Barbosa et al., 2004; Hodzic et al., 2006) resulting from a record-breaking heatwave in Europe (Luterbacher et al., 2004; Schär et al., 2004). Both forward and backward air mass trajectories calculated from HYSPLIT model support that the ELB site was potentially influenced by the intense forest fires occurred in the Southern part of Europe on the mid-August 2003 (Fig. S3), when the top altitude of the PBL was estimated to be ~4.5 km high (Hodzic et al., 2006). Although speculative, this snow layer of year 2003 peaked with rBC concentration and enriched with larger-sizes rBC particles indicates potential contribution of biomass burning aerosols transported westerly to the ELB site. This 2003 summer snow layer experienced some melting (Kozachek et al., 2016), but we can rule out that such melting was driving the unusual MMD signal described above and other snow layers with melting event did not show any anomalies of rBC MMD toward larger values. The rBC size distributions preserved in Elbrus cores could be discussed as an influence of seasonal vertical transport versus emission sources of rBC aerosols and their wet removal properties. This rBC size information is potential to provide important implications particularly for the determination of snow-melting potential by rBC particles in snow (Flanner et al., 2007; Schwarz et al., 2013). Comparison of rBC size with well-established biomass burning proxies would be required to better characterize the dependency of rBC sizes with past fire activities.

3.4 Potential emission source regions

Figure 6 illustrates potential source regions of BC aerosols reaching the ELB site. The model results show that relative to the footprints in JJA, footprints in DJF were more spread out of European continent and extended further over the Pacific (Figure 6a and b). The relative contributions of each regional footprint density over the total density are summarized in Fig. 7. Most of aerosols reaching the ELB site are transported from the European continent (WEU+CEU+EEU) accounting for 71.0 % and 55.6 % in JJA and DJF, respectively and particularly from the Eastern part of Europe (CEU+EEU) accounting for 59.0 % and 47.0 % in JJA and DJF, respectively. The region EEU brings the greatest contribution with fairly consistent features for both seasons, accounting for 35.6 % and 30.9 % in JJA and DJF, respectively. A stronger seasonality was found in the region NAF and the region NAM, where the footprint contribution was larger in DJF by a 2-fold. This seasonal variation is caused by longer particle trajectories promoted by a faster zonal flow in winter across the North Atlantic from west to east.

To investigate contributions of aerosols transporting from low altitudes which may reflect emissions at surface more sensitively, we calculated the footprint density of particles positioned in the lowest 2 km layers in the atmosphere. Note that we arbitrarily selected this vertical height of atmosphere (2 km layer) since particles positioned at lower atmosphere (e.g., ~1 km layer) was rarely observed in our simulations and the PBL heights were often higher in European mountains up to 3 km (Matthias et al., 2004). The results for JJA show that unlike in the entire atmospheric column, the contribution of footprint density from the region EEU was almost doubled in the 2 km layer, accounting for 63.6 % (Fig. 6c). Contrarily, in DJF, the proportion of the region EEU was only 22 % over total footprint density in this fixed layer. We thus infer that large seasonal increases observed during summer time in rBC mass concentration are likely driven by deposition of rBC aerosols transported from Eastern part of Europe and mostly originating from lower altitudes.

Therefore, these FLEXPART results confirm that rBC deposition to the Mt. Elbrus is most likely dominated by transport of BC emissions from the European continent, with the strongest BC inputs from the Eastern part of Europe particularly in summer.

3.5 New constrains on European BC emissions

Refractory BC concentrations of the ELB ice core increased rapidly from the 1950s to the 1980s (Figure 4 in Sect. 3.2), and such trend record should primarily reflect changes in European BC emissions (Sect. 3.4). Here, we compare past emission BC inventories with the ELB ice core record to bring new constrains on past European BC emissions.

Figure 8 shows temporal changes in anthropogenic and biomass burning BC emissions for the period 1900-2008 estimated by ACCMIP and MACCity (Diehl et al., 2012; Granier et al., 2011; Lamarque et al., 2010; van der Werf et al., 2006). The overall emission trends (black lines) illustrate a decrease of anthropogenic emissions since 1900 (Figure 8a) and a high variability of biomass burning emissions over the whole period (Figure 8b). For anthropogenic emissions, the largest BC emissions in EEU and CEU regions occurred in 1980, followed by decreasing trends. WEU had the strongest BC emissions lasting until 1960, followed by a decrease of BC emissions lasting the present-day. In 2008, anthropogenic BC emissions in region EEU, CEU and WEU are comparable with an order of 0.2 Tg yr^{-1}.

To investigate factors controlling long-term rBC trends preserved in the ELB ice core, the temporal evolution of measured ice core rBC particles can be directly compared with that of atmospheric BC load at the ELB site, at least in relative manner. This comparison is provided in Fig. 9, in which ice core record is averaged along a decadal scale to be comparable with the historic BC emission data available on decadal scale only (Lamarque et al., 2010). Specifically, we coupled the BC emission intensities in each region and their relative contribution to the entire footprint area of ELB site (Figure 8c and d). The decadal BC emission burden in each region (Figure 8a and b**)** is therefore multiplied by the contribution of footprint density (Figure 7). Assumption behind this comparison is that (i) the atmospheric circulation and transport patterns do not change with time and (ii) that the mechanisms for BC depositing on snow remained constant. Hence, the proportionality between BC mass concentration in snow and atmospheric BC load has not varied with time.

For summertime (JJA case, Fig. 9a) optimal agreement in trend pattern is observed between the ice core rBC and the atmospheric BC estimated in the lower 2 km layer with an increase at the onset of the 20th century and a subsequent decrease since ~1980 ("best scenario"). Specifically, substantial increase in atmospheric BC load is observed for the period 1910-1970, similar to the ELB rBC ice core record, only when the atmospheric BC considers BC particles transported in the lowest 2 km layer of the atmosphere. On the other side, the estimation derived from the entire atmospheric column does exhibit a different pattern. This comparison indicates that changes primarily in European anthropogenic BC emissions (e.g., industry, traffic and residential combustion), particularly ones of Eastern part of Europe, are consequently reflected in the ELB ice core rBC variability over the last century.

For wintertime (DJF case, Fig. 9b), the ice core rBC variability before 1980 can be explained by the atmospheric BC load (anthropogenic only) in the entire atmospheric column but without North American (NAM) contribution. With NAM contribution included in the simulation, the atmospheric BC is overestimated before

1980 resulting in a flat or a slightly downward trend for the period 1910-1970, unlike to the ice core rBC trend. However, the good agreement between long-term rBC changes of Greenland ice core and modeled BC deposition in Greenland using a chemistry-climate model with an input of ACCMIP BC inventory confirm that BC emission estimates for NAM from the ACCMIP inventory correctly quantify anthropogenic BC emissions in North America (Lamarque et al., 2010). Consequently, the observed overestimation of NAM contribution for winter at the ELB site (Fig 9b) is likely due to an overestimation of NAM footprint density in the statistical process applied on FLEXPART simulation data. The stronger BC inputs from NAM might have contributed to the increased winter rBC concentrations of the ELB ice core at the beginning of 20th century, although it was not shown in our simulations. Finally, the estimated BC without NAM contribution is defined as the "best scenario" for winter time.

Despite the similar features between the ice core rBC record and the best scenario for the atmospheric load which support that anthropogenic BC increase in the 20th century is reflected in the ELB record, BC maximum time period is not in total agreement (Fig. 9a and b). Unlike the ice core rBC that already largely increased in 1960 and peaked in 1970 for both summer and winter, the atmospheric BC load remarkably increases only in 1980. Substantial BC increase of ELB and Western European (CDD and CG) ice cores since the mid-20th century reveals that BC emissions increased during that period at a wide regional European scale. In addition, the CDD record shows a large increase in sulfate concentration since the mid-20th century lasting until ~1980 (Preunkert et al., 2001; Preunkert and Legrand, 2013). Knowing that sulfate and BC are often co-emitted in anthropogenic emission sources, e.g., in industrial sectors, one can expect a large increase in European BC emissions in 1960-1980, as suggested by the ELB ice core rBC record. The reliability of historic emission inventories for BC is reported to be lower than for SO_2, CO and NOx emissions, particularly for the period prior to 2000 (Granier et al., 2011), which is due to the uncertainties on BC emission factors for coal, gasoline and diesel fuels in various sectors (differ by a factor of 10 or more in literatures) and activity data (Granier et al., 2011; Vignati et al., 2010). Thus, the lack of substantial increase in the atmospheric BC load for the period 1960s-1970s could be associated primarily with underestimated European anthropogenic BC emissions for this period (Fig. 8c and d).

Moreover, the ice core rBC record and the atmospheric BC load do not exhibit similar patterns after 1980. Decreasing rates of the ice core rBC are much slower after 1980 onward for both seasons than the atmospheric BC load (Fig. 9a and b). Furthermore, the summer rBC trend of the ELB ice core even increased since 2000, although such a trend cannot be reported conclusively for winter layers (Fig. 4). The recent economic growth in Eastern, and some part of Central, European countries (World Bank Group, 2016) can contribute to the enhancement in the release of BC and co-emitted pollutants. Some of Eastern European countries have kept increasing their sulfur emissions mainly from heat production and public electricity from 2000 onward (Vestreng et al., 2007). Thus, the increase in rBC deposition at the Elbrus site, mostly identified in summer, was probably related to enhanced emissions from anthropogenic sources located in Eastern and Central Europe. On the other side, many of Eastern European countries, such as Ukraine and European part Russia which are geographically close to the Mt. Elbrus, are the countries with the greatest land use for agriculture in Europe (Rabbinge and van Diepen, 2000), and thus emissions of smoke aerosols from their agricultural waste burning are expected to be significant in summer time (Barnaba et al., 2011; Bovchaliuk et al., 2013; Stohl et al., 2007). Large emissions of smoke aerosols over Eastern Europe from summer forest/agricultural fires have been recently reported (Barnaba

et al., 2011; Bovchaliuk et al., 2013; Sciare et al., 2008; Yoon et al., 2011; Zhou et al., 2012) and burned area from Global Fire Emissions Database (GFED) (Giglio et al., 2010) increased over Eastern Europe for the period 2004-2008 (Yoon et al., 2014). These emissions of smoke aerosols in the Eastern part of Europe may have contributed to the observed summer BC increase in the ELB ice cores. Thus, the recent trend of the ELB ice core rBC turning upward probably indicates changes in both anthropogenic emissions and summer forest/peat fires over Eastern part of Europe in 2000s, which is not well reflected in the inventories.

Given the large existing uncertainties in historic BC emission inventories available to date, our rBC record reconstructed from a high-altitude Caucasus ice cores should be useful to better constrain BC emissions. Specifically, our study highlights the need for improving BC emission inventories from the Eastern part of Europe since 1960. Reliability of Western European BC emissions could be more specifically assessed by investigating high-resolution BC records extracted from Western European ice cores that would be more representative of Western European emissions.

4 Conclusions

A high-resolution rBC record reconstructed from ice cores drilled from a high-altitude Eastern European site in Mt. Elbrus (ELB), Caucasus, reported for the first time the long-term evolutions of rBC mass concentrations and size distributions in the European outflows over the past 189 years, i.e., between year 1825 and year 2013. The rBC record at ELB is largely impacted by rBC emissions located in the Eastern part of Europe. A large temporal variability in rBC mass concentration was observed at both seasonal and annual timescales. This record is also unique to document long-term variability of BC in this region of Europe.

In the first-half of 20th century, rBC concentrations increased by a 1.5-fold than its level in the preindustrial era (before 1850). The summer (winter) rBC concentrations increased by a 5-fold (3.3-fold) in 1960-1980, followed by a decrease until ~2000 and a slight increase again since ~2000. Consistent increase in background levels, since the beginning of 20th century, highlights that rBC background level in the atmosphere at ELB was also significantly altered. We have also investigated the potential of size distributions of rBC particles in the ice cores as a new proxy to bring additional information on rBC removal processes, seasonal transport patterns, and emission sources.

We simulated the atmospheric load of BC aerosols which were transported from the European continent, mainly Eastern part of Europe, by coupling transport simulations (FLEXPART) to 20th-century BC emission inventories (ACCMIP and MACCity). Similar features were observed between the ELB ice core rBC mass concentration record and the best scenario for the atmospheric BC load at the ELB site: a BC increase at the onset of the 20th century and a subsequent decrease since ~1980. This estimation evidently supports that European anthropogenic activities resulted in the BC increase over Europe since ~1900, which was also seen in elemental carbon (EC) records of Western European ice cores (Legrand et al., 2007; Thevenon et al., 2009). However, some disagreements were seen between the ELB ice core rBC and the best scenario for atmospheric BC load at ELB, e.g., (i) the lack of strong increase in the best scenario for the period 1960s and 1970s, unlike the ice core record, (ii) the different decreasing rates after 1980 and (iii) the slightly increasing trend of the rBC ELB ice core record that was not shown in the estimation. An explanation for such discrepancy could be that rapid enhancement of BC emissions over Europe since 1960 and the recent BC changes in the Eastern part of Europe may not be well

accounted for in the emission inventories.

Most atmospheric BC measurements have focused on western and northern Europe (e.g., McMeeking et al., 2010; Reche et al., 2011; Reddington et al., 2013) despite of growing evidences of strong aerosol emissions in the Eastern part of Europe (Asmi et al., 2011; Barnaba et al., 2011; Bovchaliuk et al., 2013). It is thus critically important to deploy new studies (atmospheric monitoring and investigation of ice archives) with a more comprehensive European view, including both Western and Eastern areas. We suggest that century-long ice cores at multiple high-altitude European sites with a homogeneous or well cross-compared measurement techniques are needed to better constrain past BC emissions, infer efficiency of present BC emission regulation, and help establishing future regulations on BC emissions.

Acknowledgments

This work was supported by the PEGASOS project funded by the European Commission under the Framework Programme 7 (FP7-ENV-2010-265148) and by the Russian Foundation for Basic Research (RFBR) grants 07-05-00410 and 09-05-10043. This work received funding from the French ANR programs RPD COCLICO (ANR-10-RPDOC-002-01) and the European Research Council under the European Community's Seventh Framework Program FP7/2007–2013 Grant Agreement n°291062 (project ICE&LASERS). S. Lim acknowledges support of the Korean Ministry of Education and Science Technology through a government scholarship and of the Basic Science Research Program through the National Research Foundation of Korea (NRF) funded by the Ministry of Education (2015R1A6A3A01061393). V. Mikhalenko and S. Kutuzov acknowledge support of the Russian Academy of Sciences (Department of Earth Sciences ONZ-12 Project) and RFBR grant 14-05-00137. Grateful thank to M. Zanatta for technical help in SP2 operation, S. Preunkert for technical help in ice core cutting, M. Legrand for helpful discussions, A. Berchet and J-L Bonne for help in FLEXPART simulations and N. Kehrwald for analytical help.

References

Asmi, A., Wiedensohler, A., Laj, P., Fjaeraa, A.-M., Sellegri, K., Birmili, W., Weingartner, E., Baltensperger, U., Zdimal, V., Zikova, N., Putaud, J.-P., Marinoni, A., Tunved, P., Hansson, H.-C., Fiebig, M., Kivekäs, N., Lihavainen, H., Asmi, E., Ulevicius, V., Aalto, P. P., Swietlicki, E., Kristensson, A., Mihalopoulos, N., Kalivitis, N., Kalapov, I., Kiss, G., de Leeuw, G., Henzing, B., Harrison, R. M., Beddows, D., O'Dowd, C., Jennings, S. G., Flentje, H., Weinhold, K., Meinhardt, F., Ries, L. and Kulmala, M.: Number size distributions and seasonality of submicron particles in Europe 2008–2009, Atmos. Chem. Phys., 11(11), 5505–5538, doi:10.5194/acp-11-5505-2011, 2011.

Barbosa, P., San-Miguel-Ayanz, J., Camia, A., Gimeno, M., Lib- erta, G. and Schmuck, G.: Assessment of fire damages in the EU Mediterranean Countries during the 2003 Forest Fire Campaign, Official Publication of the European Commission, Ispra., 2004.

Barnaba, F., Angelini, F., Curci, G. and Gobbi, G. P.: An important fingerprint of wildfires on the European aerosol load, Atmos. Chem. Phys., 11(20), 10487–10501, doi:10.5194/acp-11-10487-2011, 2011.

Bisiaux, M. M., Edwards, R., McConnell, J. R., Curran, M. A. J., Van Ommen, T. D., Smith, A. M., Neumann, T. A., Pasteris, D. R., Penner, J. E. and Taylor, K.: Changes in black carbon deposition to Antarctica from two high-resolution ice core records, 1850-2000 AD, Atmos. Chem. Phys., 12(9), 4107–4115, doi:10.5194/acp-12-

4107-2012, 2012a.
Bisiaux, M. M., Edwards, R., McConnell, J. R., Albert, M. R., Anschutz, H., Neumann, T. A., Isaksson, E. and Penner, J. E.: Variability of black carbon deposition to the East Antarctic Plateau, 1800-2000 AD, Atmos. Chem. Phys., 12(8), 3799–3808, doi:10.5194/acp-12-3799-2012, 2012b.
Bond, T. C., Doherty, S. J., Fahey, D. W., Forster, P. M., Berntsen, T., DeAngelo, B. J., Flanner, M. G., Ghan, S., Kärcher, B., Koch, D., Kinne, S., Kondo, Y., Quinn, P. K., Sarofim, M. C., Schultz, M. G., Schulz, M., Venkataraman, C., Zhang, H., Zhang, S., Bellouin, N., Guttikunda, S. K., Hopke, P. K., Jacobson, M. Z., Kaiser, J. W., Klimont, Z., Lohmann, U., Schwarz, J. P., Shindell, D., Storelvmo, T., Warren, S. G. and Zender, C. S.: Bounding the role of black carbon in the climate system: A scientific assessment, J. Geophys. Res. Atmos., 118(11), 5380–5552, doi:10.1002/jgrd.50171, 2013.
Bovchaliuk, A., Milinevsky, G., Danylevsky, V., Goloub, P., Dubovik, O., Holdak, A., Ducos, F. and Sosonkin, M.: Variability of aerosol properties over Eastern Europe observed from ground and satellites in the period from 2003 to 2011, Atmos. Chem. Phys., 13(13), 6587–6602, doi:10.5194/acp-13-6587-2013, 2013.
Bukowiecki, N., Weingartner, E., Gysel, M., Collaud Coen, M., Zieger, P., Herrmann, E., Steinbacher, M., Gäggeler, H. W. and and Baltensperger, U.: A Review of More Than 20 Years of Aerosol Observation at the High Altitude Research Station Jungfraujoch, Switzerland (3580masl), Aerosol Air Qual. Res., 16(3), 764–788, doi:10.4209/aaqr.2015.05.0305, 2016.
Dahlkötter, F., Gysel, M., Sauer, D., Minikin, A., Baumann, R., Seifert, P., Ansmann, A., Fromm, M., Voigt, C. and Weinzierl, B.: The Pagami Creek smoke plume after long-range transport to the upper troposphere over Europe – aerosol properties and black carbon mixing state, Atmos. Chem. Phys., 14(12), 6111–6137, doi:10.5194/acp-14-6111-2014, 2014.
Diehl, T., Heil, A., Chin, M., Pan, X., Streets, D., Schultz, M. and Kinne, S.: Anthropogenic, biomass burning, and volcanic emissions of black carbon, organic carbon, and SO2 from 1980 to 2010 for hindcast model experiments, Atmos. Chem. Phys. Discuss., 12(9), 24895–24954, doi:10.5194/acpd-12-24895-2012, 2012.
Fagerli, H., Legrand, M., Preunkert, S., Vestreng, V., Simpson, D. and Cerqueira, M.: Modeling historical long-term trends of sulfate, ammonium, and elemental carbon over Europe: A comparison with ice core records in the Alps, J. Geophys. Res., 112(D23), D23S13, doi:10.1029/2006JD008044, 2007.
Flanner, M. G., Zender, C. S., Randerson, J. T. and Rasch, P. J.: Present-day climate forcing and response from black carbon in snow, J. Geophys. Res., 112(D11), doi:Artn D11202 Doi 10.1029/2006jd008003, 2007.
Forster, C., Stohl, A. and Seibert, P.: Parameterization of Convective Transport in a Lagrangian Particle Dispersion Model and Its Evaluation, J. Appl. Meteorol. Climatol., 46(4), 403–422, doi:10.1175/JAM2470.1, 2007.
Giglio, L., Randerson, J. T., van der Werf, G. R., Kasibhatla, P. S., Collatz, G. J., Morton, D. C. and DeFries, R. S.: Assessing variability and long-term trends in burned area by merging multiple satellite fire products, Biogeosciences, 7(3), 1171–1186, doi:10.5194/bg-7-1171-2010, 2010.
Ginot, P., Dumont, M., Lim, S., Patris, N., Taupin, J.-D., Wagnon, P., Gilbert, A., Arnaud, Y., Marinoni, A., Bonasoni, P. and Laj, P.: A 10 year record of black carbon and dust from a Mera Peak ice core (Nepal): variability and potential impact on melting of Himalayan glaciers, Cryosph., 8(4), 1479–1496, doi:10.5194/tc-8-1479-2014, 2014.
Granier, C., Bessagnet, B., Bond, T. C., D'Angiola, A., Denier van der Gon, H., Frost, G. J., Heil, A., Kaiser, J.

W., Kinne, S., Klimont, Z., Kloster, S., Lamarque, J.-F., Liousse, C., Masui, T., Meleux, F., Mieville, A., Ohara, T., Raut, J.-C., Riahi, K., Schultz, M. G., Smith, S. J., Thompson, A., Aardenne, J., Werf, G. R. and Vuuren, D. P.: Evolution of anthropogenic and biomass burning emissions of air pollutants at global and regional scales during the 1980–2010 period, Clim. Change, 109(1–2), 163–190, doi:10.1007/s10584-011-0154-1, 2011.

Guilhermet, J., Preunkert, S., Voisin, D., Baduel, C. and Legrand, M.: Major 20th century changes of water-soluble humic-like substances (HULIS WS) aerosol over Europe inferred from Alpine ice cores, J. Geophys. Res. Atmos., 118(9), 3869–3878, doi:10.1002/jgrd.50201, 2013.

Hansen, J. and Nazarenko, L.: Soot climate forcing via snow and ice albedos, Proc. Natl. Acad. Sci. U. S. A., 101(2), 423–428, doi:DOI 10.1073/pnas.2237157100, 2004.

Hodzic, A., Vautard, R., Chepfer, H., Goloub, P., Menut, L., Chazette, P., Deuzé, J. L., Apituley, A. and Couvert, P.: Evolution of aerosol optical thickness over Europe during the August 2003 heat wave as seen from CHIMERE model simulations and POLDER data, Atmos. Chem. Phys., 6(7), 1853–1864, doi:10.5194/acp-6-1853-2006, 2006.

Jenk, T. M., Szidat, S., Schwikowski, M., Gaggeler, H. W., Brutsch, S., Wacker, L., Synal, H. A. and Saurer, M.: Radiocarbon analysis in an Alpine ice core: record of anthropogenic and biogenic contributions to carbonaceous aerosols in the past (1650-1940), Atmos. Chem. Phys., 6, 5381–5390, doi:10.5194/acp-6-5381-2006, 2006.

Jenkins, M., Kaspari, S., Kang, S., Grigholm, B. and Mayewski, P. A.: Black carbon concentrations from a Tibetan Plateau ice core spanning 1843–1982: recent increases due to emissions and glacier melt, Cryosph. Discuss., 7(5), 4855–4880, doi:10.5194/tcd-7-4855-2013, 2013.

Kaspari, S., Painter, T. H., Gysel, M., Skiles, S. M. and Schwikowski, M.: Seasonal and elevational variations of black carbon and dust in snow and ice in the Solu-Khumbu, Nepal and estimated radiative forcings, Atmos. Chem. Phys., 14(15), 8089–8103, doi:10.5194/acp-14-8089-2014, 2014.

Kaspari, S. D., Schwikowski, M., Gysel, M., Flanner, M. G., Kang, S., Hou, S. and Mayewski, P. A.: Recent increase in black carbon concentrations from a Mt. Everest ice core spanning 1860-2000 AD, Geophys. Res. Lett., 38, doi:Artn L04703 Doi 10.1029/2010gl046096, 2011.

Kondo, Y., Sahu, L., Moteki, N., Khan, F., Takegawa, N., Liu, X., Koike, M. and Miyakawa, T.: Consistency and Traceability of Black Carbon Measurements Made by Laser-Induced Incandescence, Thermal-Optical Transmittance, and Filter-Based Photo-Absorption Techniques, Aerosol Sci. Technol., 45(2), 295–312, doi:10.1080/02786826.2010.533215, 2011a.

Kondo, Y., Matsui, H., Moteki, N., Sahu, L., Takegawa, N., Kajino, M., Zhao, Y., Cubison, M. J., Jimenez, J. L., Vay, S., Diskin, G. S., Anderson, B., Wisthaler, A., Mikoviny, T., Fuelberg, H. E., Blake, D. R., Huey, G., Weinheimer, A. J., Knapp, D. J. and Brune, W. H.: Emissions of black carbon, organic, and inorganic aerosols from biomass burning in North America and Asia in 2008, J. Geophys. Res., 116(D8), D08204, doi:10.1029/2010JD015152, 2011b.

Kozachek, A., Mikhalenko, V., Masson-Delmotte, V., Ekaykin, A., Ginot, P., Kutuzov, S., Legrand, M., Lipenkov, V. and Preunkert, S.: Large-scale drivers of Caucasus climate variability in meteorological records and Mt Elbrus ice cores, Clim. Past Discuss., 1–30, doi:10.5194/cp-2016-62, 2016.

Laborde, M., Schnaiter, M., Linke, C., Saathoff, H., Naumann, K.-H., Möhler, O., Berlenz, S., Wagner, U., Taylor, J. W., Liu, D., Flynn, M., Allan, J. D., Coe, H., Heimerl, K., Dahlkötter, F., Weinzierl, B., Wollny, A. G., Zanatta, M., Cozic, J., Laj, P., Hitzenberger, R., Schwarz, J. P. and Gysel, M.: Single Particle Soot Photometer

625 intercomparison at the AIDA chamber, Atmos. Meas. Tech., 5, 3077–3097, doi:10.5194/amt-5-3077-2012, 2012.
626 Laborde, M., Crippa, M., Tritscher, T., Jurányi, Z., Decarlo, P. F., Temime-Roussel, B., Marchand, N., Eckhardt,
627 S., Stohl, A., Baltensperger, U., Prévôt, A. S. H., Weingartner, E. and Gysel, M.: Black carbon physical
628 properties and mixing state in the European megacity Paris, Atmos. Chem. Phys., 13(11), 5831–5856,
629 doi:10.5194/acp-13-5831-2013, 2013.
630 Lamarque, J.-F., Bond, T. C., Eyring, V., Granier, C., Heil, A., Klimont, Z., Lee, D., Liousse, C., Mieville, A.,
631 Owen, B., Schultz, M. G., Shindell, D., Smith, S. J., Stehfest, E., Van Aardenne, J., Cooper, O. R., Kainuma, M.,
632 Mahowald, N., McConnell, J. R., Naik, V., Riahi, K. and van Vuuren, D. P.: Historical (1850–2000) gridded
633 anthropogenic and biomass burning emissions of reactive gases and aerosols: methodology and application,
634 Atmos. Chem. Phys., 10(15), 7017–7039, doi:10.5194/acp-10-7017-2010, 2010.
635 Lavanchy, V. M. H., Gäggeler, H. W., Schotterer, U., Schwikowski, M. and Baltensperger, U.: Historical record
636 of carbonaceous particle concentrations from a European high-alpine glacier (Colle Gnifetti, Switzerland), J.
637 Geophys. Res. Atmos., 104(D17), 21227–21236, doi:10.1029/1999jd900408, 1999.
638 Legrand, M., Preunkert, S., Schock, M., Cerqueira, M., Kasper-Giebl, A., Afonso, J., Pio, C., Gelencsér, A. and
639 Dombrowski-Etchevers, I.: Major 20th century changes of carbonaceous aerosol components (EC, WinOC,
640 DOC, HULIS, carboxylic acids, and cellulose) derived from Alpine ice cores, J. Geophys. Res., 112(D23),
641 D23S11, doi:10.1029/2006jd008080, 2007.
642 Legrand, M., Preunkert, S., May, B., Guilhermet, J., Hoffman, H. and Wagenbach, D.: Major 20th century
643 changes of the content and chemical speciation of organic carbon archived in Alpine ice cores: Implications for
644 the long-term change of organic aerosol over Europe, J. Geophys. Res. Atmos., 118(9), 3879–3890,
645 doi:10.1002/jgrd.50202, 2013.
646 Lim, S., Faïn, X., Zanatta, M., Cozic, J., Jaffrezo, J.-L., Ginot, P. and Laj, P.: Refractory black carbon mass
647 concentrations in snow and ice: method evaluation and inter-comparison with elemental carbon measurement,
648 Atmos. Meas. Tech., 7(10), 3307–3324, doi:10.5194/amt-7-3307-2014, 2014.
649 Liu, D., Flynn, M., Gysel, M., Targino, A., Crawford, I., Bower, K., Choularton, T., Jurányi, Z., Steinbacher, M.,
650 Hüglin, C., Curtius, J., Kampus, M., Petzold, A., Weingartner, E., Baltensperger, U. and Coe, H.: Single particle
651 characterization of black carbon aerosols at a tropospheric alpine site in Switzerland, Atmos. Chem. Phys.,
652 10(15), 7389–7407, doi:10.5194/acp-10-7389-2010, 2010.
653 Lugauer, M., Baltensperger, U., Furger, M., Gäggeler, H. W., Jost, D. T., Schwikowski, M. and Wanner, H.:
654 Aerosol transport to the high Alpine sites Jungfraujoch (3454 m asl) and Colle Gnifetti (4452 m asl), Tellus B,
655 50(1), doi:10.3402/tellusb.v50i1.16026, 1998.
656 Luterbacher, J., Dietrich, D., Xoplaki, E., Grosjean, M. and Wanner, H.: European seasonal and annual
657 temperature variability, trends, and extremes since 1500., Science, 303(5663), 1499–503,
658 doi:10.1126/science.1093877, 2004.
659 Matthias, V. and Bösenberg, J.: Aerosol climatology for the planetary boundary layer derived from regular lidar
660 measurements, Atmos. Res., 63(3–4), 221–245, doi:10.1016/S0169-8095(02)00043-1, 2002.
661 Matthias, V., Balis, D., Bösenberg, J., Eixmann, R., Iarlori, M., Komguem, L., Mattis, I., Papayannis, A.,
662 Pappalardo, G., Perrone, M. R. and Wang, X.: Vertical aerosol distribution over Europe: Statistical analysis of
663 Raman lidar data from 10 European Aerosol Research Lidar Network (EARLINET) stations, J. Geophys. Res.,
664 109(D18), D18201, doi:10.1029/2004JD004638, 2004.

McConnell, J. R., Edwards, R., Kok, G. L., Flanner, M. G., Zender, C. S., Saltzman, E. S., Banta, J. R., Pasteris, D. R., Carter, M. M. and Kahl, J. D. W.: 20th-century industrial black carbon emissions altered arctic climate forcing, Science (80-.)., 317(5843), 1381–1384, doi:10.1126/science.1144856, 2007.

McMeeking, G. R., Hamburger, T., Liu, D., Flynn, M., Morgan, W. T., Northway, M., Highwood, E. J., Krejci, R., Allan, J. D., Minikin, A. and Coe, H.: Black carbon measurements in the boundary layer over western and northern Europe, Atmos. Chem. Phys., 10(19), 9393–9414, doi:10.5194/acp-10-9393-2010, 2010.

Mikhalenko, V., Sokratov, S., Kutuzov, S., Ginot, P., Legrand, M., Preunkert, S., Lavrentiev, I., Kozachek, A., Ekaykin, A., Faïn, X., Lim, S., Schotterer, U., Lipenkov, V. and Toropov, P.: Investigation of a deep ice core from the Elbrus western plateau, the Caucasus, Russia, Cryosph., 9(6), 2253–2270, doi:10.5194/tc-9-2253-2015, 2015.

Miyakawa, T., Kanaya, Y., Komazaki, Y., Taketani, F., Pan, X., Irwin, M. and Symonds, J.: Intercomparison between a single particle soot photometer and evolved gas analysis in an industrial area in Japan: Implications for the consistency of soot aerosol mass concentration measurements, Atmos. Environ., 127, 14–21, doi:10.1016/j.atmosenv.2015.12.018, 2016.

Mori, T., Moteki, N., Ohata, S., Koike, M., Goto-Azuma, K., Miyazaki, Y. and Kondo, Y.: Improved technique for measuring the size distribution of black carbon particles in liquid water, Aerosol Sci. Technol., 50(3), 242–254, doi:10.1080/02786826.2016.1147644, 2016.

Moteki, N. and Kondo, Y.: Dependence of Laser-Induced Incandescence on Physical Properties of Black Carbon Aerosols: Measurements and Theoretical Interpretation, Aerosol Sci. Technol., 44(8), 663–675, doi:10.1080/02786826.2010.484450, 2010.

Moteki, N., Kondo, Y., Oshima, N., Takegawa, N., Koike, M., Kita, K., Matsui, H. and Kajino, M.: Size dependence of wet removal of black carbon aerosols during transport from the boundary layer to the free troposphere, Geophys. Res. Lett., 39(13), doi:10.1029/2012GL052034, 2012.

Petzold, A., Ogren, J. A., Fiebig, M., Laj, P., Li, S.-M., Baltensperger, U., Holzer-Popp, T., Kinne, S., Pappalardo, G., Sugimoto, N., Wehrli, C., Wiedensohler, A. and Zhang, X.-Y.: Recommendations for reporting "black carbon" measurements, Atmos. Chem. Phys., 13(16), 8365–8379, doi:10.5194/acp-13-8365-2013, 2013.

Pio, C. A., Legrand, M., Oliveira, T., Afonso, J., Santos, C., Caseiro, A., Fialho, P., Barata, F., Puxbaum, H., Sanchez-Ochoa, A., Kasper-Giebl, A., Gelencsér, A., Preunkert, S. and Schock, M.: Climatology of aerosol composition (organic versus inorganic) at nonurban sites on a west-east transect across Europe, J. Geophys. Res., 112(D23), D23S02, doi:10.1029/2006JD008038, 2007.

Preunkert, S. and Legrand, M.: Towards a quasi-complete reconstruction of past atmospheric aerosol load and composition (organic and inorganic) over Europe since 1920 inferred from Alpine ice cores, Clim. Past, 9(4), 1403–1416, doi:10.5194/cp-9-1403-2013, 2013.

Preunkert, S., Wagenbach, D., Legrand, M. and Vincent, C.: Col du Dôme (Mt Blanc Massif, French Alps) suitability for ice-core studies in relation with past atmospheric chemistry over Europe, Tellus B, 52(3), 993–1012, doi:10.1034/j.1600-0889.2000.d01-8.x, 2000.

Preunkert, S., Legrand, M. and Wagenbach, D.: Sulfate trends in a Col du Dôme (French Alps) ice core: A record of anthropogenic sulfate levels in the European midtroposphere over the twentieth century, J. Geophys. Res. Atmos., 106(D23), 31991–32004, doi:10.1029/2001JD000792, 2001.

Rabbinge, R. and van Diepen, C. A.: Changes in agriculture and land use in Europe, Eur. J. Agron., 13(2–3), 85–

99, doi:10.1016/S1161-0301(00)00067-8, 2000.
Ramanathan, V. and Carmichael, G.: Global and regional climate changes due to black carbon, Nat. Geosci, 1(4), 221–227, 2008.
Reche, C., Querol, X., Alastuey, A., Viana, M., Pey, J., Moreno, T., Rodríguez, S., González, Y., Fernández-Camacho, R., de la Rosa, J., Dall'Osto, M., Prévôt, A. S. H., Hueglin, C., Harrison, R. M. and Quincey, P.: New considerations for PM, Black Carbon and particle number concentration for air quality monitoring across different European cities, Atmos. Chem. Phys., 11(13), 6207–6227, doi:10.5194/acp-11-6207-2011, 2011.
Reddington, C. L., McMeeking, G., Mann, G. W., Coe, H., Frontoso, M. G., Liu, D., Flynn, M., Spracklen, D. V. and Carslaw, K. S.: The mass and number size distributions of black carbon aerosol over Europe, Atmos. Chem. Phys., 13(9), 4917–4939, doi:10.5194/acp-13-4917-2013, 2013.
Schär, C., Vidale, P. L., Lüthi, D., Frei, C., Häberli, C., Liniger, M. A. and Appenzeller, C.: The role of increasing temperature variability in European summer heatwaves., Nature, 427(6972), 332–6, doi:10.1038/nature02300, 2004.
Schwarz, J. P., Gao, R. S., Fahey, D. W., Thomson, D. S., Watts, L. a., Wilson, J. C., Reeves, J. M., Darbeheshti, M., Baumgardner, D. G., Kok, G. L., Chung, S. H., Schulz, M., Hendricks, J., Lauer, a., Kärcher, B., Slowik, J. G., Rosenlof, K. H., Thompson, T. L., Langford, a. O., Loewenstein, M. and Aikin, K. C.: Single-particle measurements of midlatitude black carbon and light-scattering aerosols from the boundary layer to the lower stratosphere, J. Geophys. Res., 111(D16), D16207, doi:10.1029/2006JD007076, 2006.
Schwarz, J. P., Gao, R. S., Spackman, J. R., Watts, L. A., Thomson, D. S., Fahey, D. W., Ryerson, T. B., Peischl, J., Holloway, J. S., Trainer, M., Frost, G. J., Baynard, T., Lack, D. A., de Gouw, J. A., Warneke, C. and Del Negro, L. A.: Measurement of the mixing state, mass, and optical size of individual black carbon particles in urban and biomass burning emissions, Geophys. Res. Lett., 35(13), L13810, doi:10.1029/2008GL033968, 2008.
Schwarz, J. P., Doherty, S. J., Li, F., Ruggiero, S. T., Tanner, C. E., Perring, A. E., Gao, R. S. and Fahey, D. W.: Assessing Single Particle Soot Photometer and Integrating Sphere/Integrating Sandwich Spectrophotometer measurement techniques for quantifying black carbon concentration in snow, Atmos. Meas. Tech., 5(11), 2581–2592, doi:10.5194/amt-5-2581-2012, 2012.
Schwarz, J. P., Gao, R. S., Perring, A. E., Spackman, J. R. and Fahey, D. W.: Black carbon aerosol size in snow., Sci. Rep., 3, 1356, doi:10.1038/srep01356, 2013.
Sciare, J., Oikonomou, K., Favez, O., Markaki, Z., Liakakou, E., Cachier, H. and Mihalopoulos, N.: Long-term measurements of carbonaceous aerosols in the eastern Mediterranean: evidence of long-range transport of biomass burning, Atmos. Chem. Phys. Discuss., 8(2), 6949–6982, doi:10.5194/acpd-8-6949-2008, 2008.
Seibert, P. and Frank, a.: Source-receptor matrix calculation with a Lagrangian particle dispersion model in backward mode, Atmos. Chem. Phys., 4(1), 51–63, doi:10.5194/acp-4-51-2004, 2004.
Stephens, M., Turner, N. and Sandberg, J.: Particle identification by laser-induced incandescence in a solid-state laser cavity., Appl. Opt., 42(19), 3726–3736, 2003.
Stohl, A. and Thomson, D. J.: A Density Correction for Lagrangian Particle Dispersion Models, Boundary-Layer Meteorol., 90(1), 155–167, doi:10.1023/A:1001741110696, 1999.
Stohl, A., Forster, C., Frank, A., Seibert, P. and Wotawa, G.: Technical note: The Lagrangian particle dispersion model FLEXPART version 6.2, Atmos. Chem. Phys., 5(9), 2461–2474, doi:10.5194/acp-5-2461-2005, 2005.
Stohl, A., Berg, T., Burkhart, J. F., Fjæraa, A. M., Forster, C., Herber, A., Hov, Ø., Lunder, C., McMillan, W. W.,

Oltmans, S., Shiobara, M., Simpson, D., Solberg, S., Stebel, K., Ström, J., Tørseth, K., Treffeisen, R., Virkkunen, K. and Yttri, K. E.: Arctic smoke – record high air pollution levels in the European Arctic due to agricultural fires in Eastern Europe in spring 2006, Atmos. Chem. Phys., 7(2), 511–534, doi:10.5194/acp-7-511-2007, 2007.

Taylor, J. W., Allan, J. D., Allen, G., Coe, H., Williams, P. I., Flynn, M. J., Le Breton, M., Muller, J. B. A., Percival, C. J., Oram, D., Forster, G., Lee, J. D., Rickard, A. R., Parrington, M. and Palmer, P. I.: Size-dependent wet removal of black carbon in Canadian biomass burning plumes, Atmos. Chem. Phys., 14(24), 13755–13771, doi:10.5194/acp-14-13755-2014, 2014.

Thevenon, F., Anselmetti, F. S., Bernasconi, S. M. and Schwikowski, M.: Mineral dust and elemental black carbon records from an Alpine ice core (Colle Gnifetti glacier) over the last millennium, J. Geophys. Res., 114, doi:D17102 10.1029/2008jd011490, 2009.

Tørseth, K., Aas, W., Breivik, K., Fjæraa, A. M., Fiebig, M., Hjellbrekke, A. G., Lund Myhre, C., Solberg, S. and Yttri, K. E.: Introduction to the European Monitoring and Evaluation Programme (EMEP) and observed atmospheric composition change during 1972–2009, Atmos. Chem. Phys., 12(12), 5447–5481, doi:10.5194/acp-12-5447-2012, 2012.

Tsyro, S., Simpson, D., Tarrasón, L., Klimont, Z., Kupiainen, K., Pio, C. and Yttri, K. E.: Modeling of elemental carbon over Europe, J. Geophys. Res., 112(D23), D23S19, doi:10.1029/2006JD008164, 2007.

Venzac, H., Sellegri, K., Villani, P., Picard, D. and Laj, P.: Seasonal variation of aerosol size distributions in the free troposphere and residual layer at the puy de Dôme station, France, Atmos. Chem. Phys., 9(4), 1465–1478, doi:10.5194/acp-9-1465-2009, 2009.

Vestreng, V., Myhre, G., Fagerli, H., Reis, S. and Tarrasón, L.: Twenty-five years of continuous sulphur dioxide emission reduction in Europe, Atmos. Chem. Phys., 7(13), 3663–3681, doi:10.5194/acp-7-3663-2007, 2007.

Vignati, E., Karl, M., Krol, M., Wilson, J., Stier, P. and Cavalli, F.: Sources of uncertainties in modelling black carbon at the global scale, Atmos. Chem. Phys., 10(6), 2595–2611, doi:10.5194/acp-10-2595-2010, 2010.

Wang, M., Xu, B., Kaspari, S. D., Gleixner, G., Schwab, V. F., Zhao, H., Wang, H. and Yao, P.: Century-long record of black carbon in an ice core from the Eastern Pamirs: Estimated contributions from biomass burning, Atmos. Environ., 115, 79–88, doi:10.1016/j.atmosenv.2015.05.034, 2015.

Wendl, I. A., Menking, J. A., Färber, R., Gysel, M., Kaspari, S. D., Laborde, M. J. G. and Schwikowski, M.: Optimized method for black carbon analysis in ice and snow using the Single Particle Soot Photometer, Atmos. Meas. Tech. Discuss., 7(3), 3075–3111, doi:10.5194/amtd-7-3075-2014, 2014.

van der Werf, G. R., Randerson, J. T., Giglio, L., Collatz, G. J., Kasibhatla, P. S. and Arellano, A. F.: Interannual variability in global biomass burning emissions from 1997 to 2004, Atmos. Chem. Phys., 6(11), 3423–3441, doi:10.5194/acp-6-3423-2006, 2006.

van der Werf, G. R., Randerson, J. T., Giglio, L., Collatz, G. J., Mu, M., Kasibhatla, P. S., Morton, D. C., DeFries, R. S., Jin, Y. and van Leeuwen, T. T.: Global fire emissions and the contribution of deforestation, savanna, forest, agricultural, and peat fires (1997–2009), Atmos. Chem. Phys., 10(23), 11707–11735, doi:10.5194/acp-10-11707-2010, 2010.

World Bank Group, M.: The World Bank Data, 2016.

Xu, Y., Ramanathan, V. and Washington, W. M.: Observed high-altitude warming and snow cover retreat over Tibet and the Himalayas enhanced by black carbon aerosols, Atmos. Chem. Phys., 16(3), 1303–1315, doi:10.5194/acp-16-1303-2016, 2016.

Yoon, J., von Hoyningen-Huene, W., Vountas, M. and Burrows, J. P.: Analysis of linear long-term trend of aerosol optical thickness derived from SeaWiFS using BAER over Europe and South China, Atmos. Chem. Phys., 11(23), 12149–12167, doi:10.5194/acp-11-12149-2011, 2011.

Yoon, J., Burrows, J. P., Vountas, M., von Hoyningen-Huene, W., Chang, D. Y., Richter, A. and Hilboll, A.: Changes in atmospheric aerosol loading retrieved from space-based measurements during the past decade, Atmos. Chem. Phys., 14(13), 6881–6902, doi:10.5194/acp-14-6881-2014, 2014.

Yttri, K. E., Aas, W., Bjerke, A., Cape, J. N., Cavalli, F., Ceburnis, D., Dye, C., Emblico, L., Facchini, M. C., Forster, C., Hanssen, J. E., Hansson, H. C., Jennings, S. G., Maenhaut, W., Putaud, J. P. and Tørseth, K.: Elemental and organic carbon in PM10: a one year measurement campaign within the European Monitoring and Evaluation Programme EMEP, Atmos. Chem. Phys., 7(22), 5711–5725, doi:10.5194/acp-7-5711-2007, 2007.

Zhou, C., Penner, J. E., Flanner, M. G., Bisiaux, M. M., Edwards, R. and McConnell, J. R.: Transport of black carbon to polar regions: Sensitivity and forcing by black carbon, Geophys. Res. Lett., 39(22), L22804, doi:10.1029/2012gl053388, 2012.

Table and figures

Tables

Table 1. rBC mass concentrations at seasonal resolution and relative increases compared to 1825-1850 (preindustrial era) for different time periods.

Time period	Summer		Winter	
	Concentration in μg L^{-1} (median ± SD)	Relative increase to 1825-1850	Concentration in μg L^{-1} (median ± SD)	Relative increase to 1825-1850
1825-1850	4.3±1.5	1.0	2.0±0.9	1.0
1850-1900	5.3±2.6	1.1	2.5±1.4	1.0
1900-1950	7.9±3.9	1.5	3.2±1.6	1.4
1950-2000	20.0±7.1	4.3	6.0±2.7	2.7
1960-1980	22.6±7.2	5.0	7.1±2.5	3.3
2000-2013	17.7±5.9	3.9	5.4±2.3	2.4

Figure captions

Figure 1. Location of the ice core drilling site (43°20'53, 9"N, 42°25'36, 0"E, 5115 m a.s.l., indicated by the red star or arrow) in the Mt. Elbrus, the western Caucasus mountain range between the Black and the Caspian seas.

Figure 2. Five sub-regions classified as potential rBC emission source regions. Elbrus drilling site is indicated by a red circle. WEU, CEU, EEU, NAF and NAM represent Western Europe, Central Europe, Eastern Europe, North Africa and North America, respectably.

Figure ~~3~~3. A Profile of high-resolution rBC concentration of Mt. Elbrus ice cores. (a) whole rBC profile of both the 2013 core and the 2009 core, and (b) the 2009 core from top to 20 m corresponding to the blue region in (a). In (b), lower resolution (at ~5-10 cm resolution; black color) and high resolution (at 1 cm resolution; red color) rBC profiles obtained from discrete analysis and continuous flow analysis, respectively, are shown. For a whole rBC record, a section of lower-resolution signals of the 2009 core (corresponding to calendar year 2009) was replaced with the high-resolution rBC signals of the 2013 core. Gray text on top of figures stands for calendar year corresponding to ice core depth.

Figure 4. Annually averaged temporal evolution in rBC mass concentration of the ELB ice cores. (a) Summer, (b) winter, and (c) annual variabilities. Thin solid line is medians and dashed lines are lower and upper 10^{th} percentiles of the seasonal or annual rBC values. Upper 10^{th} percentiles do not exceed 75 μg L^{-1}, 35 μg L^{-1}, and 56 μg L^{-1} for summer, winter, and annual, respectively. Thick lines are 10-year smoothing of medians. Discontinuous thin lines indicate ice layers with unclear seasonality or unanalyzed ice layers. Note different y-scales for three time series of rBC concentrations.

Figure 5. Time series of mass mode diameter (MMD) of seasonal rBC size distributions for the period of 1940-2009. The MMD was obtained by fitting a log-normal curve to the measured distribution. Horizontal lines stand for geometric means for summer (red) and winter (blue).

Figure 6. Air mass footprint area for (a) June to August (JJA) and (b) December to February (DJF) in the atmospheric column and (c) JJA in the lowest 2 km in the atmosphere. Color bar on the left indicates footprints density with a process defined unit (p.d.u.). The location of the ELB site is marked by a white triangle. JJA and DJF correspond to summer and winter of the ELB ice core depth, respectively.

Figure 7. Contribution of each regional footprint density (%) for (a) JJA and (b) DJF in the atmospheric column and (c) JJA in the lowest 2 km in the atmosphere. Footprint density of each region is divided by the footprint density of the entire footprint area (EEU+CEU+WEU+NAF+NAM+Others) and then described in percentage. Information for each region is found in the Sect. 2.4.

Figure 8. Historic regional BC emissions and atmospheric BC load at ELB for the period 1900-2008. In (a) and (b), anthropogenic and biomass burning (forest fires and savanna burning) BC emissions estimated by ACCMIP and MACCity (Diehl et al., 2012; Granier et al., 2011; Lamarque et al., 2010; van der Werf et al., 2006). In (c) and (d), atmospheric BC load (Tg yr^{-1}) is calculated by multiplying decadal-scale BC emissions in each region (a and b) by its relative contribution to the entire footprint area of ELB site (figure 7). In (c), both anthropogenic and biomass burning emissions are used for the reconstruction in JJA, as this type of biomass burning (forest fires and savanna burning) is the most frequent in summer and in (d), only anthropogenic emissions are used for DJF. Details are found in the text.

Figure 9. Comparison in temporal evolution between the rBC mass concentration of the ELB ice core and the estimates of atmospheric BC load at the ELB site, on a decadal scale. (a) JJA and (b) DJF. Best scenarios for

atmospheric BC load are shown in black thick lines. In (b), NAM stands for North America. See the text and Figure 8c and d for calculations of the atmospheric BC load.

Figures

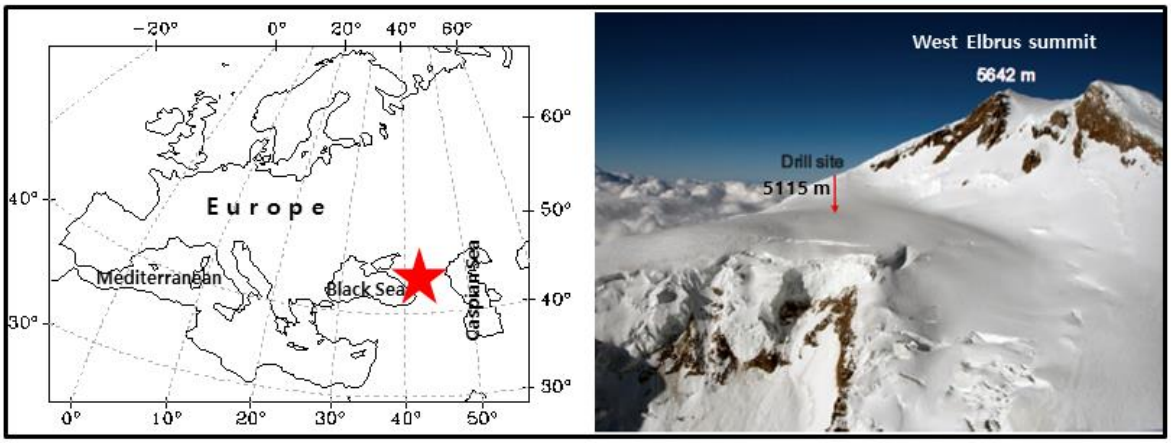

Figure 1

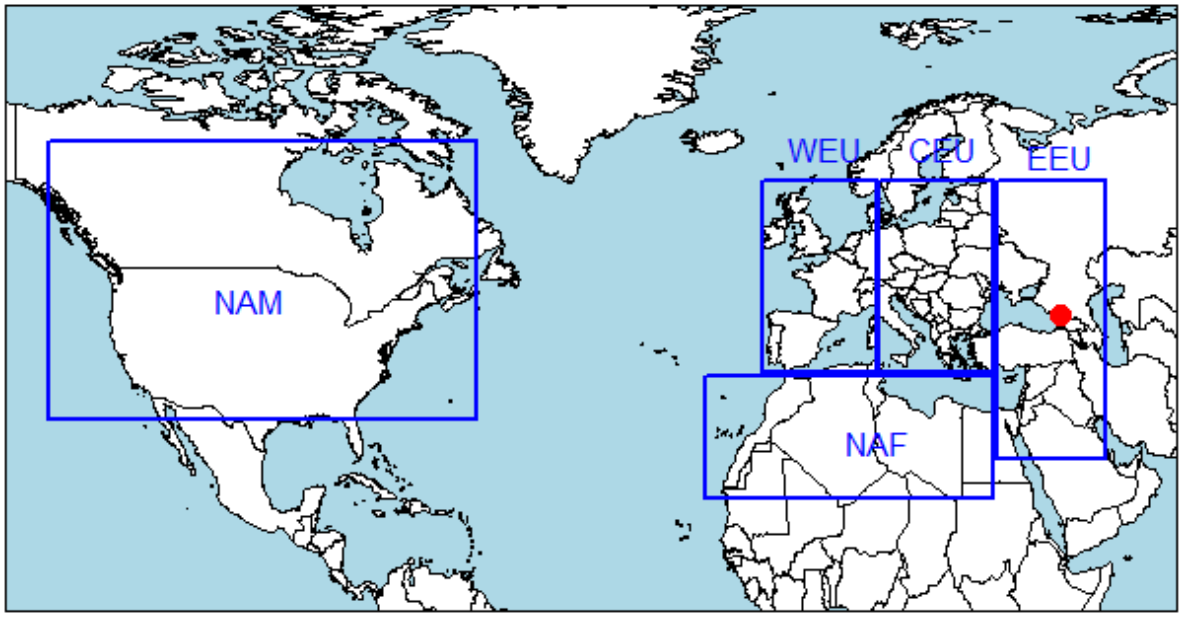

Figure 2

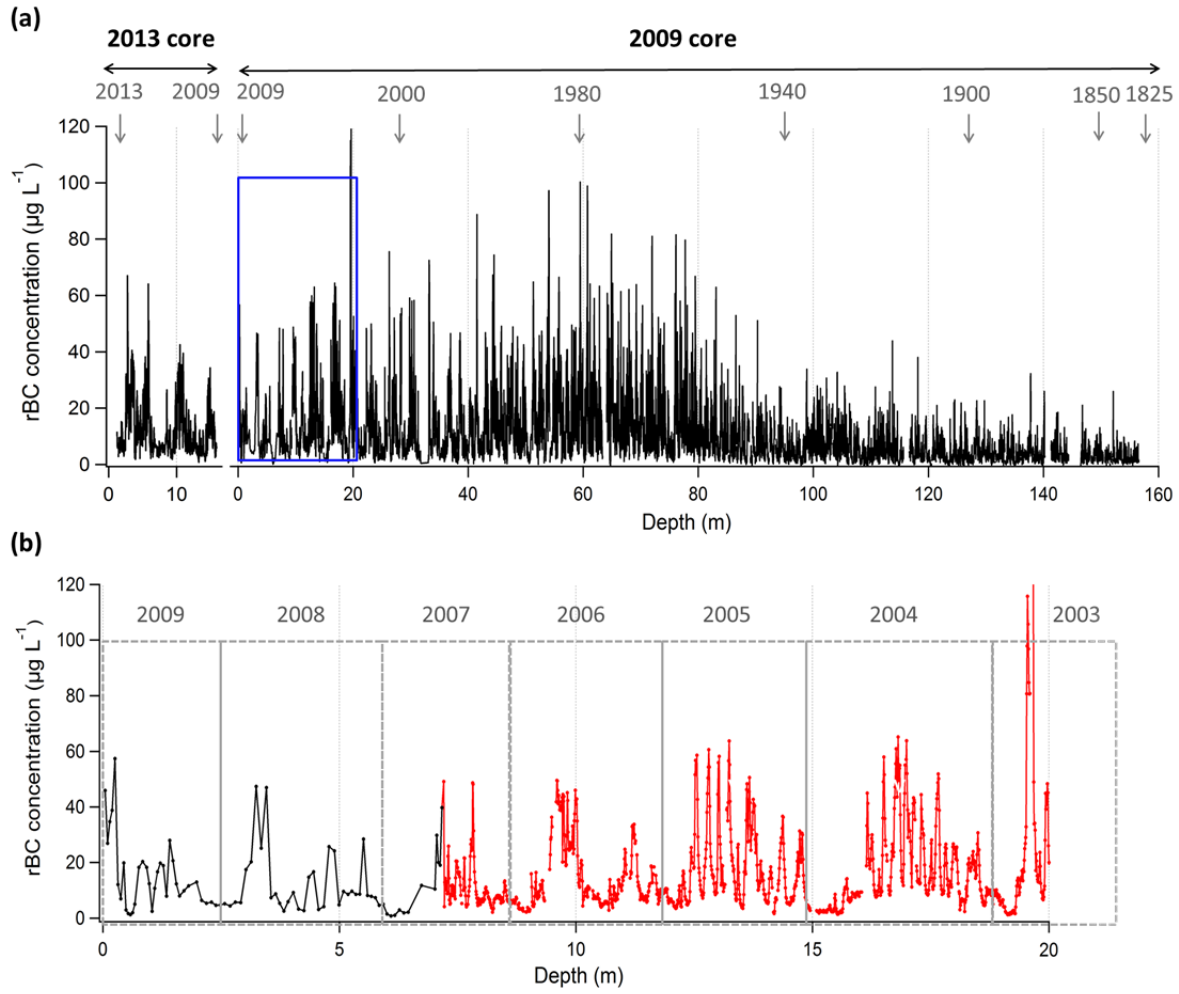
(a)
2013 core
2009 core
2013
2009
2009
2000
1980
1940
1900
1850
1825
rBC concentration (µg L-1)
Depth (m)
(b)
2009
2008
2007
2006
2005
2004
2003
rBC concentration (µg L-1)
Depth (m)

Figure 3

927 **(a)**

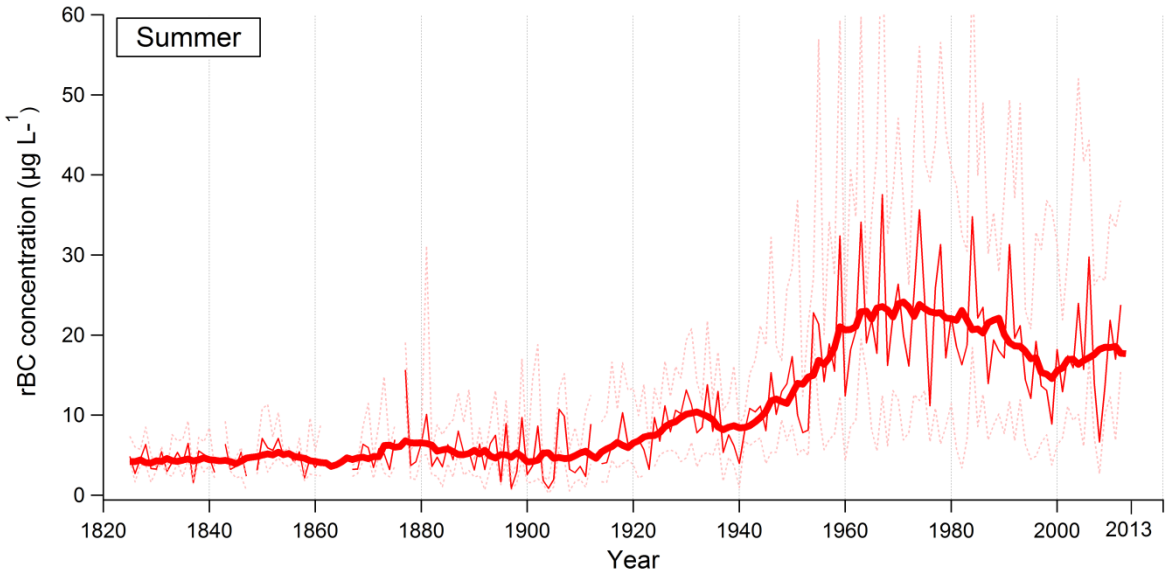

928

929

930 **(b)**

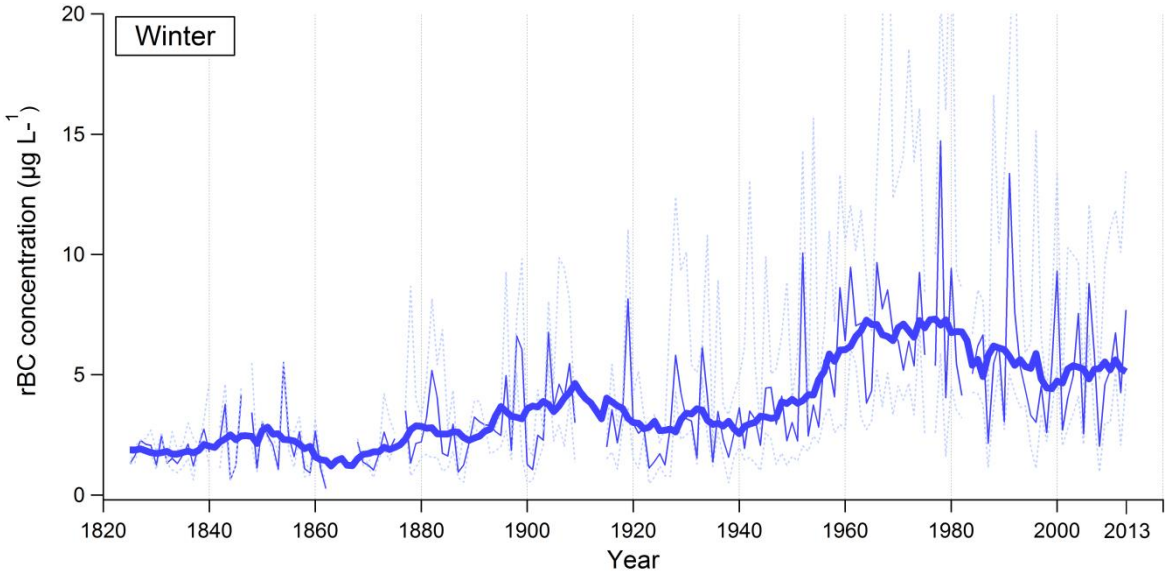

931

932

933 **(c)**

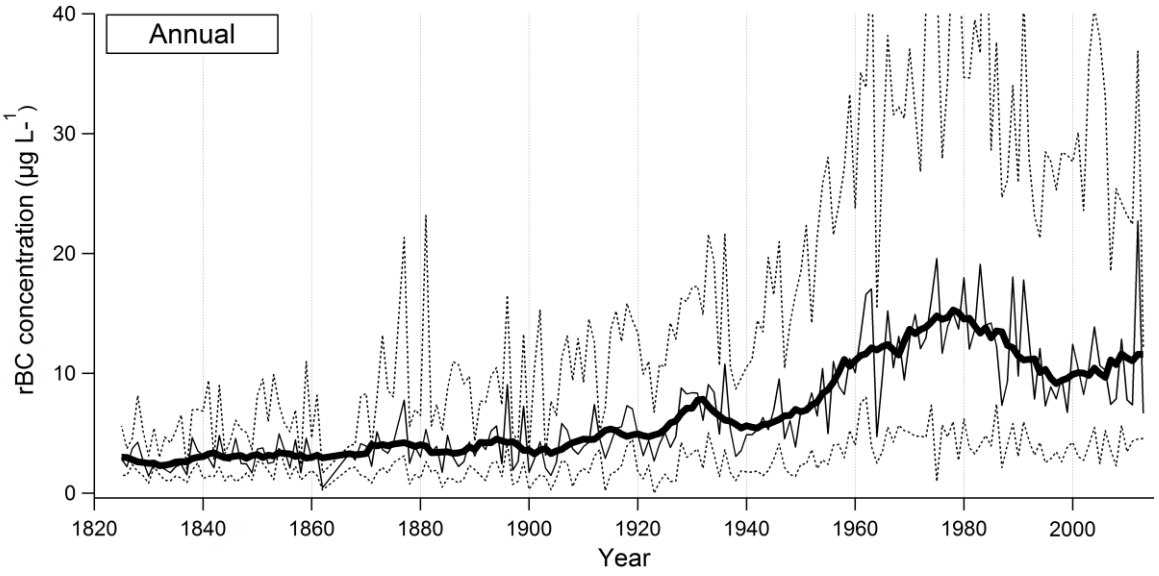

Figure 4

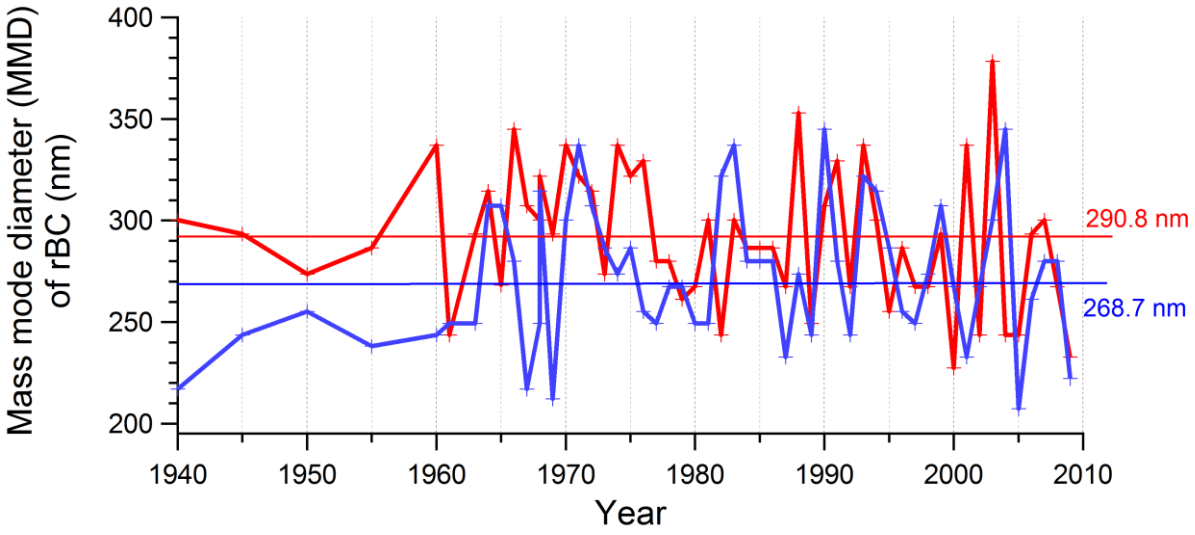

Figure 5

(a) **(b)**

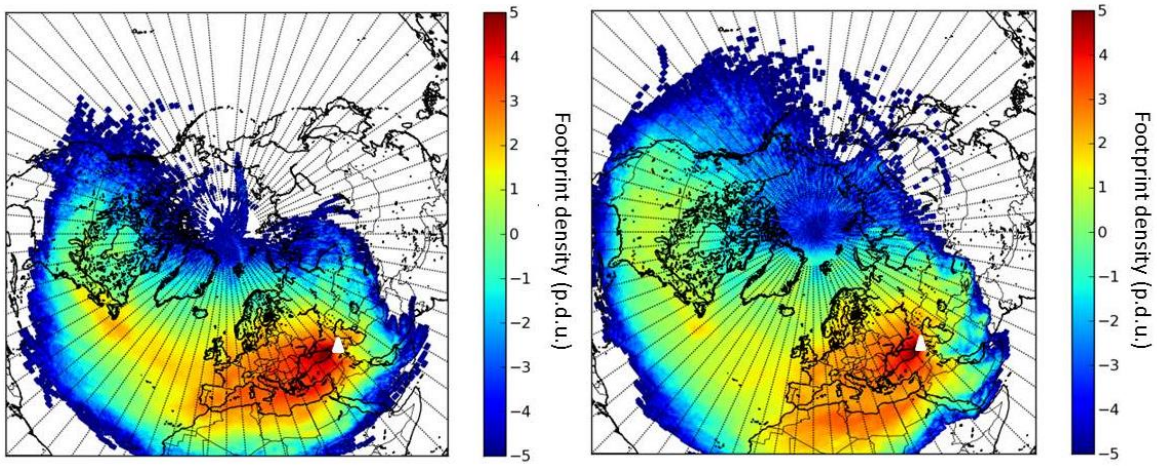
5
4
3
2
1
0
−1
−2
−3
−4
−5
Footprint density (p.d.u.)
5
4
3
2
1
0
−1
−2
−3
−4
−5
Footprint density (p.d.u.)

(c)

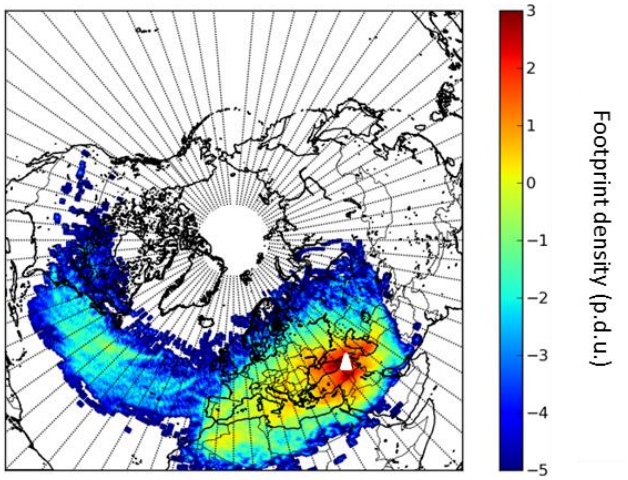
3
2
1
0
−1
−2
−3
−4
−5
Footprint density (p.d.u.)

Figure 6

968 **(a)**

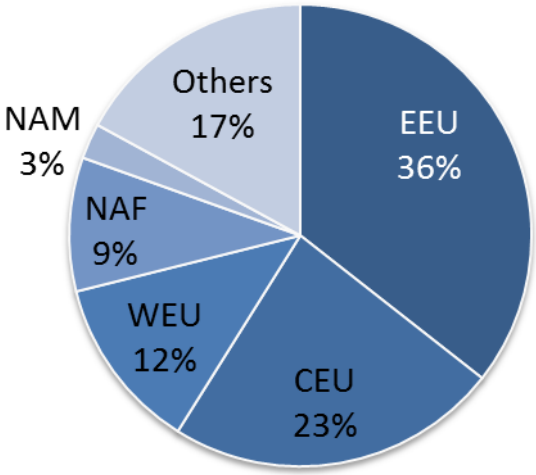

969 **(b)**

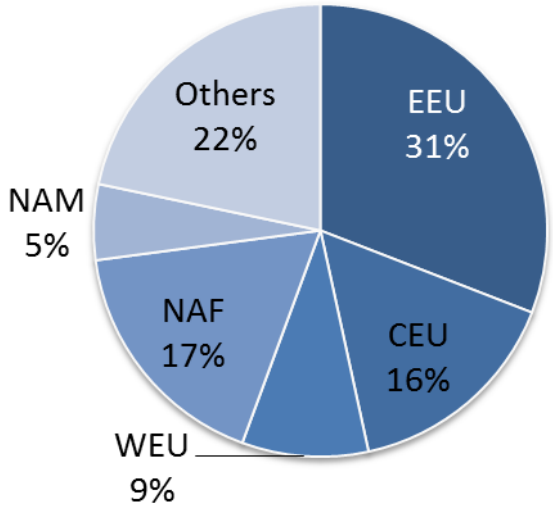

970

(c)

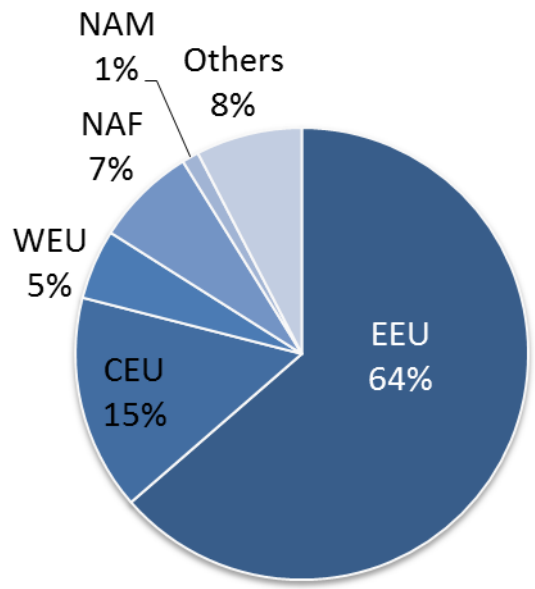

Figure 7

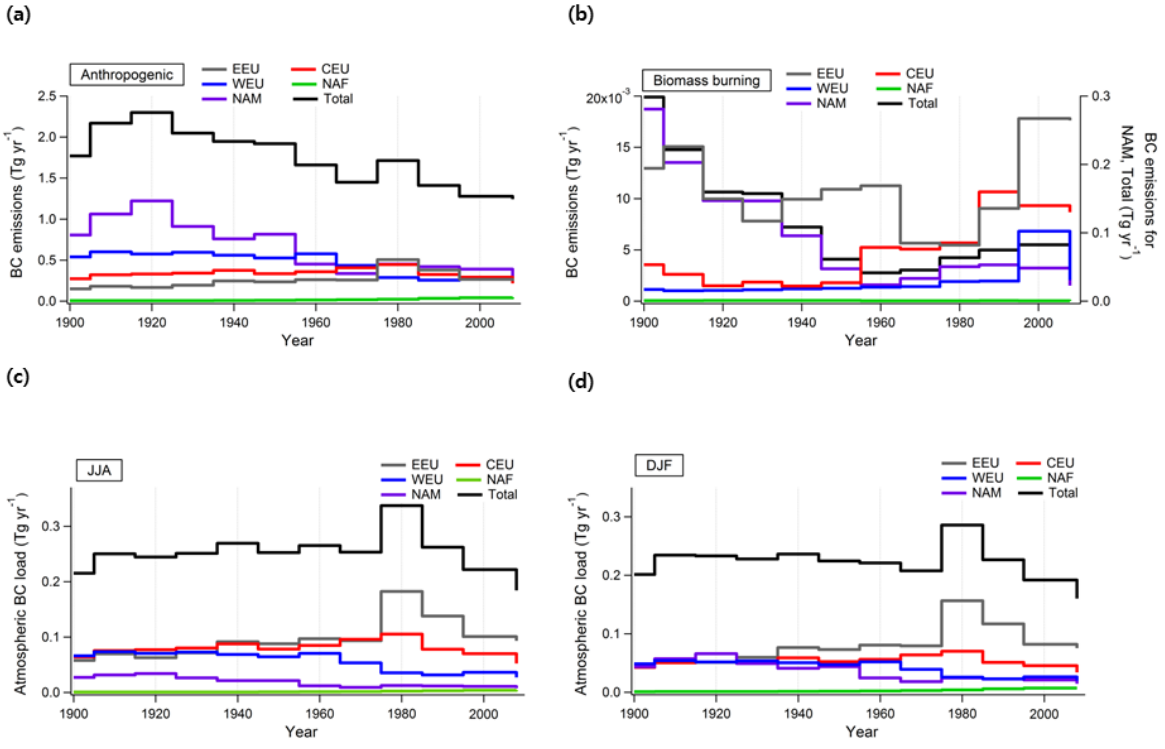

Figure 8

(a)

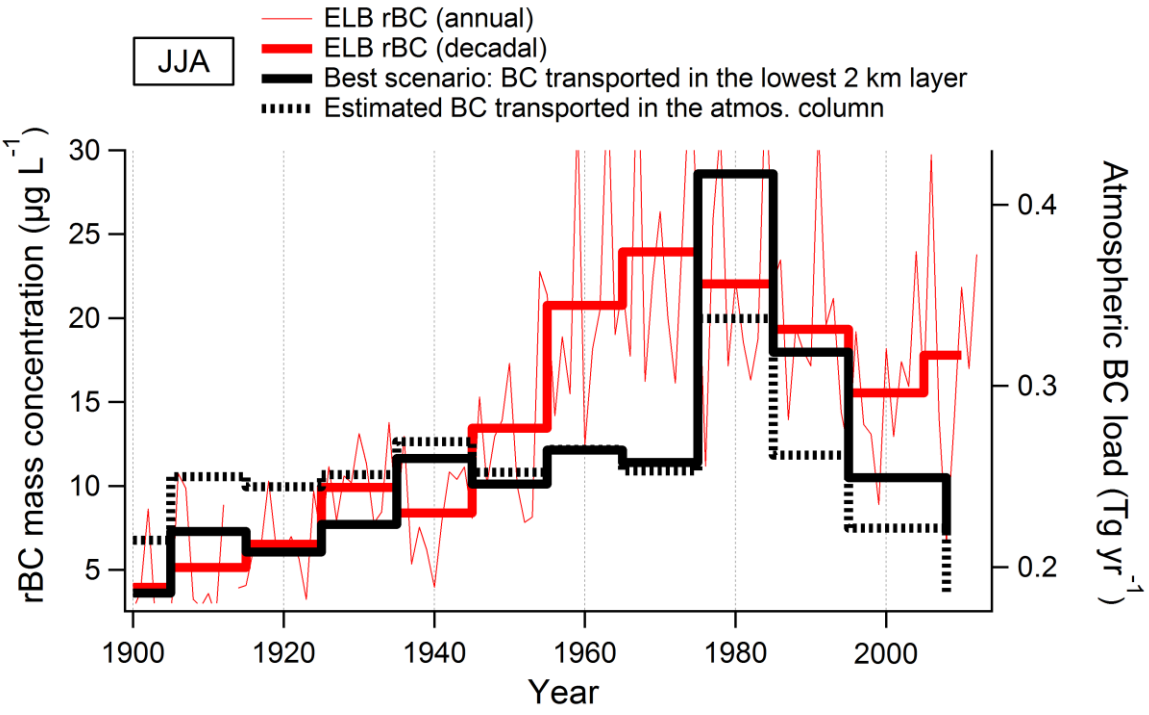
JJA
ELB rBC (annual)
ELB rBC (decadal)
Best scenario: BC transported in the lowest 2 km layer
Estimated BC transported in the atmos. column
rBC mass concentration (μg L-1)
Atmospheric BC load (Tg yr-1)
Year
1900
1920
1940
1960
1980
2000
5
10
15
20
25
30
0.2
0.3
0.4

(b)

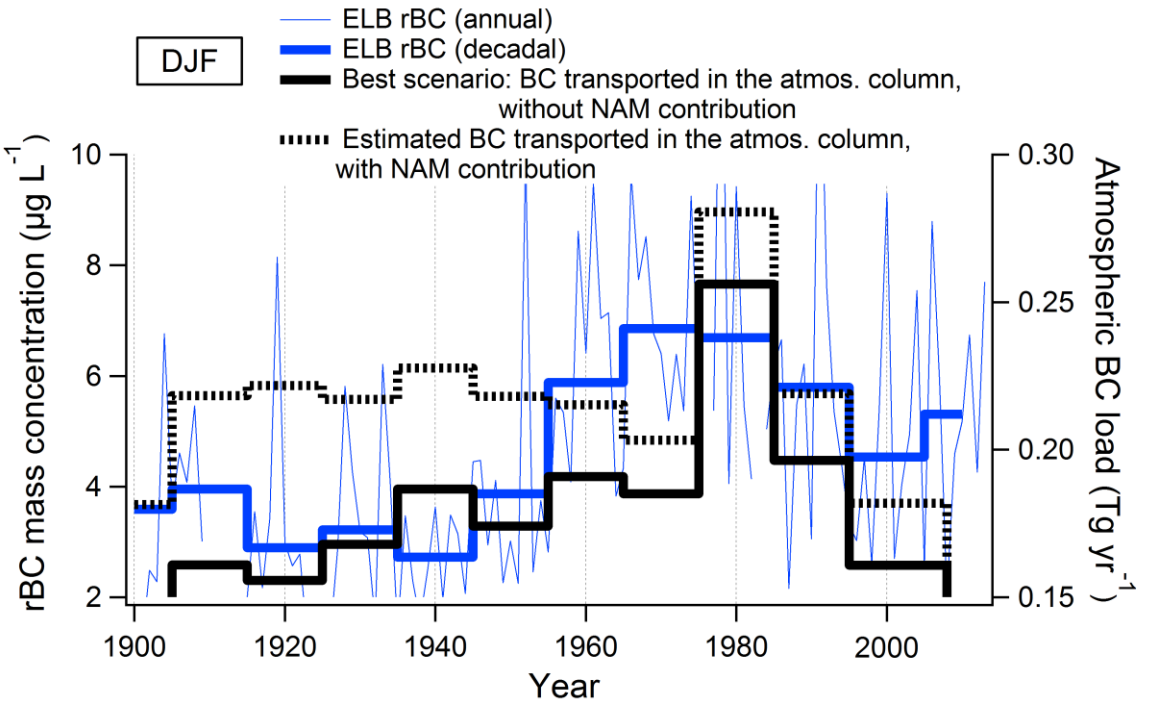
DJF
ELB rBC (annual)
ELB rBC (decadal)
Best scenario: BC transported in the atmos. column, without NAM contribution
Estimated BC transported in the atmos. column, with NAM contribution
rBC mass concentration (μg L-1)
Atmospheric BC load (Tg yr-1)
Year
1900
1920
1940
1960
1980
2000
2
4
6
8
10
0.15
0.20
0.25
0.30

Figure 9